Dalton Transactions

ROYAL SOCIETY OF CHEMISTRY

PERSPECTIVE

View Article Online
View Journal | View Issue

Cite this: *Dalton Trans.*, 2024, **53**, 15764

Polarized metal–metal multiple bonding and reactivity of phosphinoamide-bridged heterobimetallic group IV/cobalt compounds

Nathanael H. Hunter and Christine M. Thomas *

Heterobimetallic complexes are studied for their ability to mimic biological systems as well as active sites in heterogeneous catalysts. While specific interest in early/late heterobimetallic systems has fluctuated, they serve as important models to fundamentally understand metal–metal bonding. Specifically, the polarized metal–metal multiple bonds formed in highly reduced early/late heterobimetallic complexes exemplify how each metal modulates the electronic environment and reactivity of the complex as a whole. In this Perspective, we chronicle the development of phosphinoamide-supported group IV/cobalt heterobimetallic complexes. This combination of metals allows access to a low valent Co^{-I} center, which performs a rich variety of bond activation reactions when coupled with the pendent Lewis acidic metal center. Conversely, the low valent late transition metal is also observed to act as an electron reservoir, allowing for redox processes to occur at the d^0 group IV metal site. Most of the bond activation reactions carried out by phosphinoamide-bridged M/Co^{-I} (M = Ti, Zr, Hf) complexes are facilitated by cleavage of metal–metal multiple bonds, which serve as readily accessible electron reservoirs. Comparative studies in which both the number of buttressing ligands as well as the identity of the early metal were varied to give a library of heterobimetallic complexes are summarized, providing a thorough understanding of the reactivity of M/Co^{-I} heterobimetallic systems.

Received 17th July 2024,
Accepted 20th August 2024

DOI: 10.1039/d4dt02064b

rsc.li/dalton

Introduction

To quote the late Prof. Malcolm Chisholm, "Anything one can do, two can do too – and it's more interesting."[1] The expansion of coordination compounds to contain more than one transition metal center represents a rapidly intensifying area of interest in inorganic chemistry. Such bimetallic complexes have been used to study metal–metal cooperativity,[2–10] and to give insight into the activity of both metalloenzymes[11–15] and heterogeneous catalysts.[16,17] The two metals in a bimetallic complex need not be directly linked *via* a metal–metal bond, but can be held in close proximity by a dinucleating or bridging ligand framework. For example, the dithiolate-bridged Ni–Fe and Ni–Pd complexes published by Darensbourg *et al.*[18–21] are an excellent showcase of heterobimetallic biomimetic activity and open the door to the discussion of many novel and interesting site-differentiated multimetallic metal clusters and their widespread reactivity.[22–25] However, this Perspective will instead more narrowly focus on early/late heterobimetallic complexes with direct polarized interactions between the two metals and the reactivity unique to such metal–metal bonds. In particular, the authors hope to provide a personal account of the development of phosphinoamide-linked early/late heterobimetallic compounds featuring metal–metal multiple bonds and their reactivity patterns, in hopes of providing fundamental insight into the structure/function relationships that correlate metal–metal bonding and reactivity.

Department of Chemistry and Biochemistry, The Ohio State University, 100 W, 18th Ave, Columbus, OH 43210, USA. E-mail: thomasc@chemistry.ohio-state.edu

Overview of metal–metal bonding

First, an introduction to metal–metal bonds, particularly those between first-row metals, is warranted. It would be a travesty to start a discussion about metal–metal bonding without crediting the late F. A. Cotton.[26] While the covalency of single bonds between metals had been studied,[27,28] and metal–metal multiple bonding had been postulated,[29] it was Cotton *et al.* that first discovered examples of metal–metal double,[30] triple,[31] and quadruple bonds,[32] all with tetrachlororhenate(III)-based systems. These discoveries sparked thousands of reports of metal–metal multiple bonds,[4,26,33–43] but the hypothetical metal–metal quintuple bond remained elusive until the first Cr–Cr quintuple bond was reported by Power *et al.* in 2005.[44] To aid in quantifying the degree of metal–metal bonding

using structural parameters alone, Cotton developed a metric known as the Formal Shortness Ratio (FSR).[26] The FSR of a multimetallic molecule is defined as the distance between two metal centers divided by the sum of the single bond atomic radii (Pauling's R_1)[45] of each metal atom component. This definition is sufficiently general to be applied for comparative purposes across a broad range of systems with different metal–metal combinations and allows a general correlation between bond length and bond order, even among heterobimetallic complexes. However, distance alone is not sufficient to describe the covalent interactions between two metal centers as there is a broad variance in FSR between metal–metal bonds of different orders.[26] As an example, Power's Cr–Cr quintuple-bonded complex has a metal–metal distance (1.8351 (4) Å, FSR = 0.77) that is comparable to many of the previously reported Cr–Cr quadruple-bonded complexes.[26,44] It is for this reason that analysis of the electronic structure is also required to provide a complete understanding of metal–metal bonding from an orbital overlap perspective.

The degree of metal–metal bonding in bimetallic complexes is dependent upon the local symmetry of each metal and the d orbital population dictated by each metal's formal oxidation state. For example, Fig. 1 depicts the differences in orbital configuration and population as well as metal–metal bond order as a function of symmetry and orbital population. In a hypothetical ligandless low-spin bimetallic Cr^ICr^I dication (Fig. 1, left), a maximum bond order of five could be obtained,

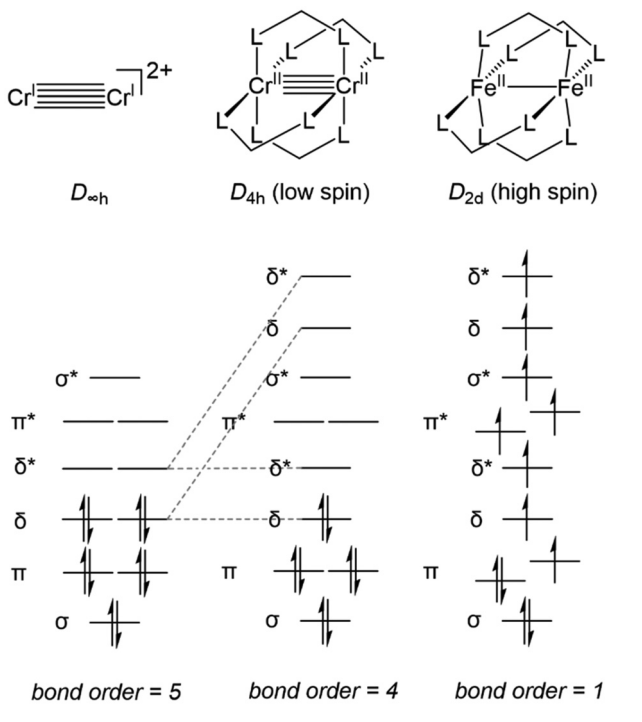

Fig. 1 A comparison of the frontier molecular orbitals and metal–metal bond order of an idealized $D_{\infty h}$ metal–metal quintuple-bonded system, a low spin D_{4h} paddlewheel complex, and a high spin D_{2d} paddlewheel complex. L^L represents a dinucleating monoanionic ligand.

thus inspiring the low-coordination number in Power's Cr–Cr quintuple bond. More commonly, multiple dinucleating ligands are employed to support bimetallic systems. Bimetallic systems of D_{4h} symmetry are the most ubiquitous, and carboxylate, triazenate, or amidinate bridging ligands have been used to form "paddlewheel" $[M_2L_4]$ complexes with most of the first-row transition metals, including vanadium,[46–52] chromium,[50,53,54] iron,[55,56] cobalt,[57–60] nickel,[61–65] and copper,[61,66,67] with metal–metal bond orders ranging from 0 to 4. In D_{4h} symmetry the degeneracy of the δ orbitals is broken, resulting in population of δ* antibonding orbitals in compounds with more than 8d electrons and a maximum bond order of 4 (Fig. 1, middle). Moreover, the high-spin configurations of many first row bimetallic complexes result in lower bond orders due to the population of multiple M–M antibonding orbitals (Fig. 1, right).[33,56] In the diiron paddlewheel case, the high spin configuration also leads to a Jahn–Teller distortion from D_{4h} to D_{2d} symmetry. Heterobimetallic paddlewheels have also been reported, such as the example reported by Tonks *et al.* wherein (2-diphenylphosphido)pyrrolide linkers aid in the formation of a Ti–Fe triple bond.[68]

Lower symmetry trigonal D_{3h} and C_{3v} systems do not suffer from the "early" population of antibonding orbitals owing to the weaker C_3-symmetric ligand field and maintained degeneracy of the orbitals of δ symmetry (Fig. 2A), and have been shown to support metal–metal multiple bonding among first-row transition metals and in heterobimetallic systems.[4,33,60,69] Many different C_3-symmetric ligand systems have been utilized to develop early/late heterobimetallic complexes.[69,70,71,7233] Multiple bonds are common with these systems not only due to their favorable symmetry, but also because of their electronic properties. The Lewis acidic nature of the early transition metal serves to withdraw electron density from the late transition metal *via* metal–metal dative donor–acceptor interactions, which results in more facile reduction.[33] Upon reduction, the atomic orbitals of the late transition metal rise in energy, resulting in more orbital overlap and an increase in metal–metal bond order. Orbitals of the proper symmetry to form metal–metal δ bonds are often populated in reduced early/late heterobimetallic compounds. However, due to the differences in electronegativity and orbital energies of the two metals, these orbitals, which also have poor spatial overlap, typically remain non-bonding and localized on each metal (Fig. 2B).

Metal–metal bonding in early/late heterobimetallic complexes

Interest in early/late heterobimetallic complexes has fluctuated since the 1980s,[2,73–77] initially inspired by efforts to mimic the so-called "strong metal–support interactions" observed between late transition metal catalysts and metal oxide supports such as titania.[17,78,79] Within this research area, there are several particularly noteworthy examples of early/late heterobimetallic compounds featuring polarized metal–metal bonds. While not formally assigned as a metal–metal multiple bond, the bonding between titanium and iron in Gade's HC $(Me_2SiNTol)_3TiFe(CO)_2Cp$ (**A**) compound was described as a

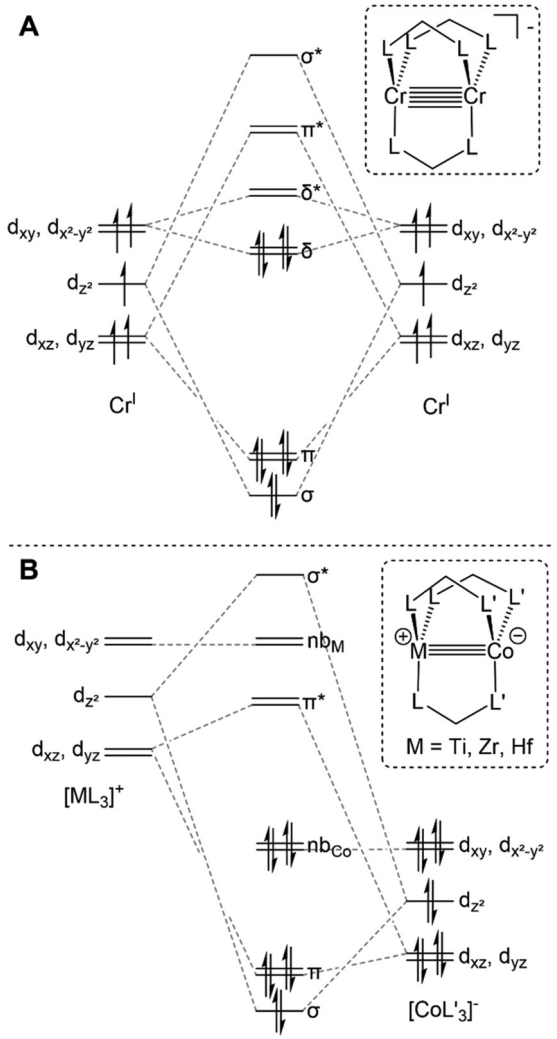

Fig. 2 Qualitative molecular orbital diagrams depicting the metal–metal bonding in representative trigonal homobimetallic (A) and early/late heterobimetallic (B) complexes. L^L represents a bidentate monoanionic ligand that is either symmetric (A) or asymmetric (B) with different donor types.

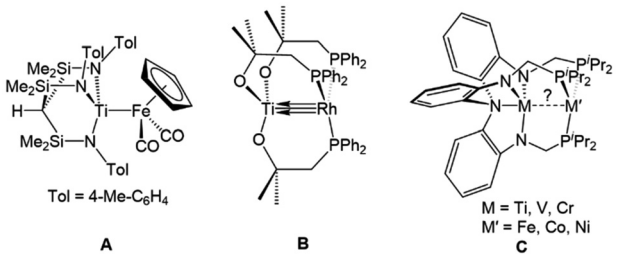

Fig. 3 Selected examples of early/late heterobimetallic complexes featuring metal–metal (multiple) bonds reported by Gade (**A**),[80] Wolczanski (**B**),[70] and Lu (**C**).[72]

combination of donor–acceptor interactions with both σ and π character (Fig. 3), demonstrating that there is a driving force for such interactions in the absence of bridging ligands.[80]

Wolczanski *et al.* leveraged the hard/soft acid/base preferences of alkoxyphosphine ligands to stabilize multiple bonds between group IV metals and late transition metals.[70,81–84] For example, the C_3 symmetric Ti/Rh heterobimetallic complex Ti$(OC(CH_3)_2CH_2PPh_2)_3$Rh (**B**) was found to have a record-breaking short Ti–Rh distance of 2.2142(11) Å (FSR = 0.86) (Fig. 3).[70] A computational investigation found that the metal–metal bonding consisted of three (one σ and two π) well-defined polarized dative bonds that Wolczanski chose to represent using a solid line and two arrows. We have adopted a similar depiction of bonding to represent both bond order and the donor/acceptor qualities of the metal–metal interactions throughout this Perspective and in most of our published work.

The examples most closely related to those discussed herein are a series of C_3-symmetric trigonal lantern complexes studied by Lu and coworkers utilizing the heptadentate "double-decker" ligand $[N(o\text{-}(NCH_2P^iPr_2)C_6H_4)_3]^{3-}$.[72,85] A series of late transition metal Ti/M,[86] V/M,[87] and Cr/M [88–90] complexes (M = Fe, Co, Ni) were investigated, with several metal–metal pairs giving rise to metal–metal multiple bonding in their fully reduced states (**C**, Fig. 3).[72] Similar systems using the double-decker ligand motif to link late transition metals with main group metals and lanthanides have given rise to catalytic systems for carbon dioxide reduction to formate,[91–93] the hydrogenation of alkenes and alkynes,[94,95] and the hydrodefluorination of aryl fluorides.[96]

These examples reported by Wolczanski and Lu illustrate the utility of heterobifunctional ligands with a hard anionic donor and a soft neutral donor, which preferentially bind to high-valent early metals and low-valent late metals, respectively. This binding site differentiation is key to stabilizing two disparate metals in a single framework, leading to the facile formation of metal–metal multiple bonds.

Phosphinoamide-linked early/late heterobimetallic complexes

The first examples of early/late heterobimetallic complexes linked by phosphinoamide ligands were reported by Nagashima and coworkers.[97–100] In contrast to the ligands described above, phosphinoamide ligands feature two distinct coordination sites (amide and phosphine) directly joined through a single covalent bond. This ensures that the two metal centers are held in close proximity, promoting orbital overlap and metal–metal interactions. Combining early metal phosphinoamide compounds with late transition metal precursors, heterobimetallic bis(phosphinoamide) and tris(phosphinoamide) compounds such as $Cl_2Ti(^tBuNPPh_2)_2PtX_2$ (**D**, X = Cl, Me), $[Cl_2Ti(^tBuNPPh_2)_2M(\eta^3\text{-allyl})]^+$ (**E**, M = Ni, Pd, Pt), $ClZr(^iPrNPPh_2)_3Mo(CO)_3$ (**F**), and $ClZr(^iPrNPPh_2)_3CuCl$ (**G**) were synthesized (Fig. 4).[97–100] The cationic Ti/M allyl complexes **E** were found to be active catalysts for allylic amination reactions, and the authors found that the appended Lewis acidic Ti center increased the electrophilicity of the M-allyl fragment and was crucial for achieving catalysis, as monometallic Ni, Pd, and Pt phosphine complexes with similar structures were unable to achieve catalytic turnover.[98]

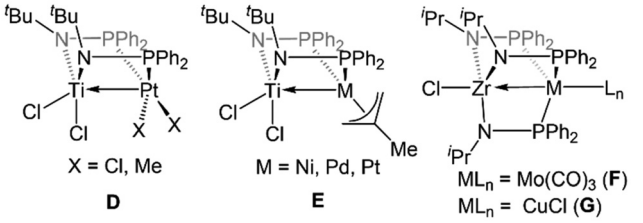

Fig. 4 Phosphinoamide-linked heterobimetallic complexes reported by Nagashima and coworkers.[97–100]

Drawing inspiration from the precedents set by Nagashima *et al.*, our group set out to synthesize a wider variety of phosphinoamide-supported early/late heterobimetallic complexes and explore their redox properties and reactivity. Using three phosphinoamide ligands to bridge an early and late metal gives the previously discussed C_3 symmetry about the bimetallic core. The trigonal ligand field and the proximity of the two metal centers facilitated the construction of early/late heterobimetallic complexes bearing metal–metal multiple bonds.[33,71] We have reported a wide variety of tris(phosphinoamide) and bis(phosphinoamide) early/late heterobimetallics using late first-row transition metals, including Cr/M,[101] V/M,[102–104] Nb/M,[105–107] Ti/M,[104] and U/Co[108] combinations (M = Fe, Co, Ni, Cu). However, the most heavily studied metal–metal combinations to date are the group IV M/Co complexes (M = Ti, Zr, Hf) and that is where we will focus this Perspective. Trends in metal–metal bonding will be described in the context of the unique reactivity enabled by these compounds and their polarized metal–metal multiple bonds and enhanced redox behavior.

Zr/Co (phosphinoamide) complexes

Metal–metal bonding in tris(phosphinoamide) Zr/Co complexes

The Zr/Co pair initially sparked our interest owing to the availability of multiple common oxidation states ranging from Co^{III} to Co^{-I} for cobalt, combined with the relative inertness of zirconium to redox processes. The tendency of Zr to remain in the d^0 Zr^{IV} state was initially posited (and later confirmed)[109] to lend simplicity to the assignment of redox processes to one metal or the other while ensuring that the Lewis acidity of the early metal center remains unperturbed by redox events alone. Our foray into tris(phosphinoamide) complexes began in 2009, when our group reported a series of three Zr^{IV}/Co^{I} tris(phosphinoamide) compounds, each distinguished by the substituents on the amide and phosphine donors, ClZr(^{i}PrNPPh$_2$)$_3$CoI (**1**), ClZr(MesNP^{i}Pr$_2$)$_3$CoI (**2**), and ClZr(^{i}PrNP^{i}Pr$_2$)$_3$CoI (**3**) (Mes = 2,4,6-trimethylphenyl, Fig. 5).[110] The metal–metal distances in **1–3** range from 2.73 Å (**1**) to 2.63 Å (**2** and **3**), corresponding to FSRs of 1.00–1.04, and the metal–metal bonding in these compounds is best described as a dative Co→Zr bond. Cyclic voltammetry experiments demonstrated that the potentials for one and two-electron reduction of the Co(I) center in bimetallic complex **1** decreased by 0.84 and 1.01 V, respectively, as compared to a Co monometallic species with an otherwise identical coordination environment about the Co center, (^{i}PrNHPPh$_2$)$_3$CoI. Even the most electron-donating variant of the ligand set (**3**) could be reduced at potentials more than 0.5 V more positive than the aforementioned monometallic Co species. This seminal discovery demonstrated the remarkable impact of a Lewis acidic early metal ion in facilitating redox processes at an appended late metal center, demonstrating the utility of early/late heterobimetallic frameworks for accessing highly reduced and reactive species.

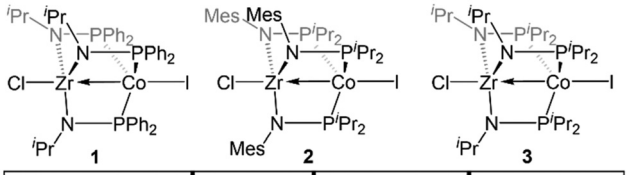

	1	2	3
Zr-Co distance (Å)	2.7315(5)	2.6280(5)	2.6309(5)
FSR[a]	1.04	1.00	1.00

Fig. 5 Tris(phosphinoamide) linked Zr^{IV}/Co^{I} compounds featuring dative Co→Zr bonds. [a] FSR is defined as the ratio of the metal–metal distance to the sum of the single bond atomic radii of the two metals.

Complexes **1–3** readily undergo two-electron reduction, affording dinitrogen-bound Zr^{IV}/Co^{-I} species when reduced under a dinitrogen atmosphere.[110,111] The PPh_2-substituted complex **1** is reduced to afford an anionic complex [{ClZr(^{i}PrNPPh$_2$)$_3$CoN$_2$}$_2$Na(THF)$_4$][Na(THF)$_6$] (**4**) that retains the Zr-bound halide (Fig. 6). Although high quality single crystal X-ray diffraction data could not be obtained for **4**, its formulation and connectivity were inferred by comparison of its

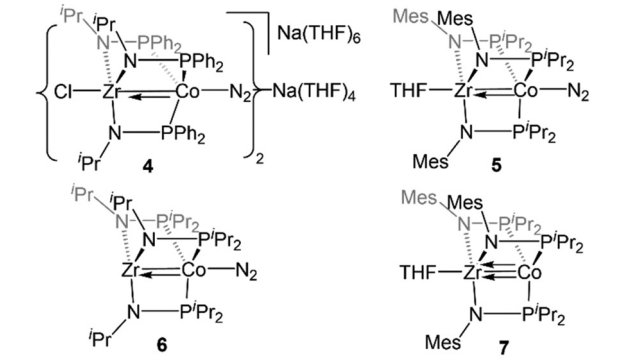

	5	6	7
Zr-Co distance (Å)	2.3649(18)	2.328(3)	2.1432(13)
FSR[a]	0.90	0.89	0.82

Fig. 6 Tris(phosphinoamide) linked Zr^{IV}/Co^{-I} compounds featuring metal–metal multiple bonds. [a] FSR is defined as the ratio of the metal–metal distance to the sum of the single bond atomic radii of the two metals.

spectroscopic features to a Hf/Co analogue (*vide infra*).[112] In contrast, the two P^{i}Pr$_2$-substituted compounds **2** and **3** generate zwitterionic species (THF)Zr(MesNP^{i}Pr$_2$)$_3$CoN$_2$ (**5**) and Zr(^{i}PrNP^{i}Pr$_2$)$_3$CoN$_2$ (**6**) *via* loss of two equivalents of sodium halide salt (Fig. 6).[111] Reduction products **5** and **6** feature Zr–Co distances that are dramatically shortened upon reduction, with FSRs of 0.90 and 0.89, respectively. Complex **2** can be reduced in the absence of dinitrogen to afford the N$_2$-free complex (THF)Zr(MesNP^{i}Pr$_2$)$_3$Co (**7**), which has an even shorter Zr–Co distance (2.1432(13) Å, FSR = 0.82).[111]

A computational analysis of the frontier molecular orbitals of **5–7** revealed that the decrease in metal–metal distance results from an increase in Zr–Co bond order upon reduction. A representative frontier molecular orbital diagram of **7** is shown in Fig. 7A, revealing a metal–metal triple bond comprised of one σ bonding orbital and two π bonding orbitals. All three metal–metal bonding orbitals are polarized, with significantly more orbital contribution from the Co center. The two highest occupied molecular orbitals are Co-centered d_{xy} and $d_{x^2-y^2}$ orbitals of δ-symmetry. Although the formation of metal–metal δ bonds is symmetry-allowed, δ-bonding is inherently weaker as a result of poorer orbital overlap and, due to the energy differences between the Zr and Co atomic orbitals, δ bonding is negligible in these heterobimetallic systems. The net result is a $(\sigma)^2(\pi)^4(Co_{nb})^4$ electronic configuration and a metal–metal triple bond in **7** (Fig. 7A).[33,109,111,113] Although the d_{xz} and d_{yz} orbitals in Zr^{IV}/Co^{I} complex **2** were also of the correct symmetry to form metal–metal π bonds, such bonding interactions only form upon reduction of the cobalt center to Co^{-I}, as this raises the energy of the cobalt-centered orbitals such that overlap with the higher energy d_{xz} and d_{yz} orbitals on Zr becomes possible. Due to the highly reduced nature of the cobalt center in **7** and its C_3 symmetry, the d_{xz} and d_{yz} orbitals on cobalt are also of the proper symmetry and energy to bind dinitrogen, generating **5** upon exposure to N$_2$. Examination of the frontier molecular orbitals shows that although the $(\sigma)^2(\pi)^4(Co_{nb})^4$ electronic configuration is retained in **5**, significant mixing of the M–M π bonding orbitals with the dinitrogen π* orbitals decreases the metal–metal orbital overlap and results in a bond order closer to two (Fig. 7B).[111] As a result of competition between Zr and N$_2$ for the electron density in Co's d_{xz} and d_{yz} orbitals, the apical dinitrogen ligand in **5** is rather labile and samples of **5** revert to **7** *in vacuo*.[111] The oxidation states of compounds **5–7** are best described as Zr^{IV}/Co^{-I} and therefore these compounds undergo a myriad of oxidative chemistry,[109] facilitated by the open coordination sites or labile ligands on both the Zr and Co apical sites.

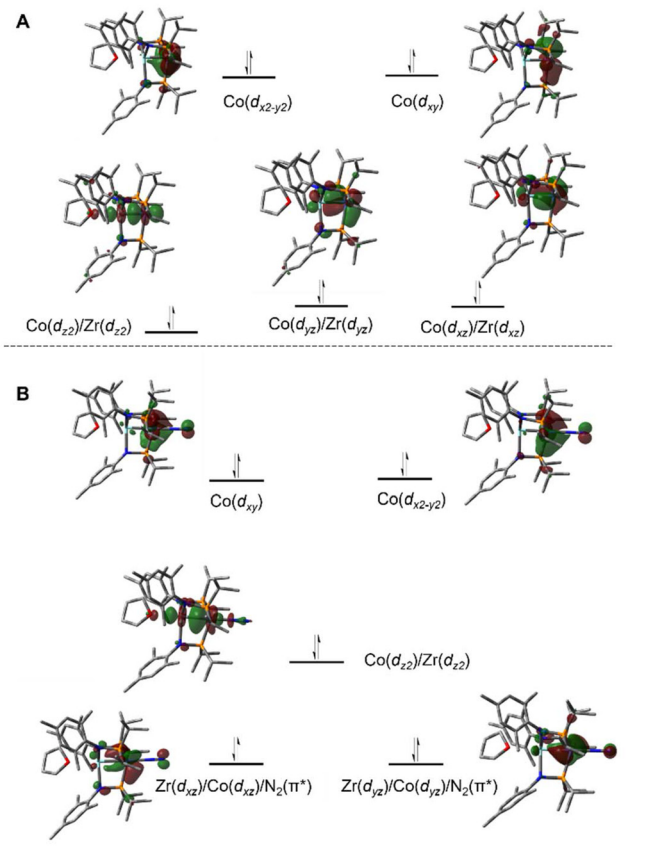

Fig. 7 Pictorial representations of the frontier MO diagrams of **7** (A) and **5** (B) derived from DFT calculations (ωB97XD/def2SVP).

Reactivity of tris(phosphinoamide) Zr/Co complexes

Oxidative addition across the Zr–Co bond. Simple two-electron redox processes are less common at first-row transition metal centers than with their heavier noble metal congeners. However, oxidative addition across the metal–metal multiple bonds in phosphinoamide-linked Zr^{IV}/Co^{-I} complexes occurs readily (Scheme 1). Exposure of **5** to I$_2$ results in a two-electron oxidative addition across the Zr–Co bond to form the diiodide complex (η^2-^{i}Pr$_2$PNMes)Zr(μ-MesNP^{i}Pr$_2$)$_2$(μ-I)CoI (**8**).[114] In **8**, one of the phosphinoamide ligands dissociates from Co and binds η^2 to the Zr center to accommodate the bridging iodide ligand. This hemilabile ligand behavior was conserved in the reaction of **5** with MeI to generate the methyl-bridged complex (η^2-^{i}Pr$_2$PNMes)Zr(μ-MesNP^{i}Pr$_2$)$_2$(μ-CH$_3$)CoI (**9**). Attempts to oxi-

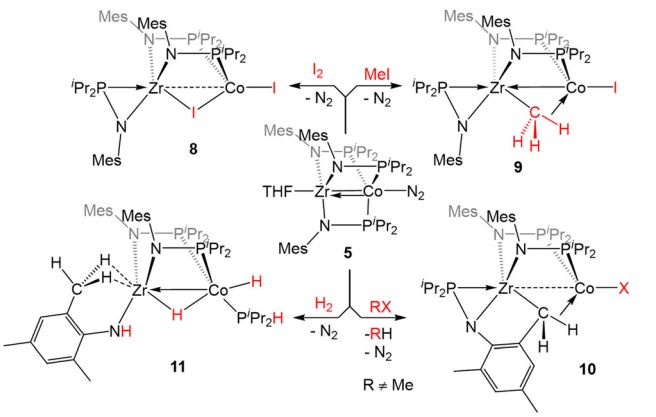

Scheme 1 Examples of two-electron oxidative addition reactions of **5**.

datively add other alkyl halides to **5** resulted in intramolecular C–H activation of one of the mesityl methyl groups and formation of **10** with concomitant release of alkane.[115] Complex **5** also oxidatively adds H_2 across its Zr/Co bond; however, H_2 addition was accompanied by the cleavage of the N–P bond of one of the phosphinoamide ligands to form **11**.[115]

The propensity of reduced tris(phosphinoamide) Zr^{IV}/Co^{-I} species for C–X bond activation was harnessed for catalytic Kumada coupling reactions of alkyl halides with alkyl Grignard reagents.[116] Through computational mechanistic studies, it was found that the extremely reducing nature of the $[ZrCo]^{3+}$ bimetallic core enables the catalysis, as the lowest energy pathway begins with a net oxidative addition achieved by a one-electron reduction of the alkyl halide followed by a radical recombination event with the resulting open-shell Zr^{IV}/Co^{0} intermediate.[117] The Zr^{IV}/Co^{I} oxidative addition product then undergoes transmetallation with the alkyl Grignard reagent, a phosphine dissociation event, and subsequent reductive elimination to form a C–C bond and regenerate the Zr^{IV}/Co^{-I} catalyst.[117] The bimetallic nature of the Zr/Co system was also found to favor reductive elimination *via* the withdrawal of electron density from Co by the neighboring Lewis acidic Zr^{IV} center. Neither the oxidative addition, nor the reductive elimination were found to be energetically accessible with a cobalt monometallic analogue.[117]

Complex **5** was also found to readily oxidatively add the C–H bonds of terminal alkynes. When exposed to two equivalents of TMSC≡CH or PhC≡CH at low temperatures, an adduct of the *E*-isomer of the dimerized enyne was formed (**12**, Scheme 2).[118] Although TMSC≡CH addition to **5** led to exclusive formation of the *E*-isomer, even at room temperature, all three potential enyne isomers (*E*, *Z*, and *gem*) were generated when the addition of PhC≡CH to **5** was carried out at room temperature. It was hypothesized, and later determined computationally,[119] that this reaction takes place *via* an initial oxidative addition of the terminal C–H bond of the alkyne, followed by insertion of a second equivalent of alkyne into the resulting cobalt hydride bond, and then reductive elimination to arrive at the enyne adduct. This mechanism was supported by trapping a C–H activated bridging acetylide intermediate, (η^2-$^{i}Pr_2$PNMes)Zr(μ-MesNP^{i}Pr$_2$)$_2$(μ-C≡CTMS)Co(H)(CN^{t}Bu) (**13**), *via* the addition of ^{t}BuNC to the mixture of TMSC≡CH to **5**.[118]

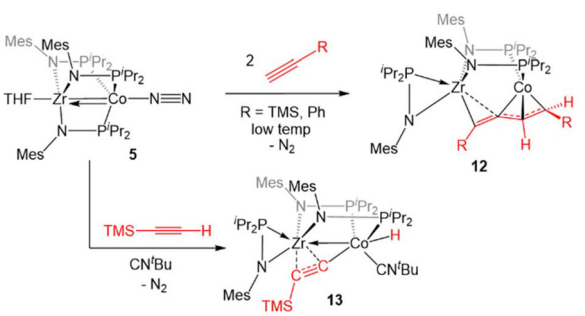

Scheme 2 Reactions of terminal alkynes with **5**.

One-electron *vs.* two-electron processes in E–H and E–E bond activation (E = N, S, O). In addition to C–H activation, Zr^{IV}/Co^{-I} complex **5** was found to activate the N–H bonds of hydrazine derivatives. Treatment of **5** with 1.5 equivalents of hydrazine or a monosubstituted hydrazine derivative resulted in the one-electron oxidation of the complex and the binding of an η^2 hydrazido ligand at the Zr site to form Zr^{IV}/Co^{0} products (η^2-RNNH$_2$)Zr(MesNP^{i}Pr$_2$)$_3$Co(N$_2$) (R = H (**14^{H}**), Ph (**14^{Ph}**), Me (**14^{Me}**)). These one-electron processes require formal loss of H$^{\bullet}$ and were found to concomitantly generate 0.5 equiv. NH_3 and 0.5 equiv. of RNH_2 through H$^{\bullet}$-promoted cleavage of the N–N bond of an additional 0.5 equiv. of the hydrazine derivative (Scheme 3). Of note, **14^{H}** serves as the first example of an unsubstituted η^2 hydrazido ligand bound to Zr. When two equivalents of phenylhydrazine are added to **5**, hydrazido formation is also accompanied by an addition of a phenyl aminyl radical at cobalt in an overall two-electron process to generate (η^2-RNNH$_2$)Zr(MesNP^{i}Pr$_2$)$_3$Co(NHPh) (**15**), supporting the proposed radical mechanism (Scheme 3).[120]

The reactivity of **5** with sulfur-containing substrates was also investigated (Scheme 3). The reaction between **5** and two equivalents of thiophenol or one equivalent of diphenyl disulfide yielded Zr^{IV}/Co^{I} product (η^2-MesNP^{i}Pr$_2$)Zr(μ-MesNP^{i}Pr$_2$)$_2$(μ-SPh)Co(SPh) (**16**).[121] A similar oxidative process occurred with excess diethyl peroxide but with the conservation of the C_3 symmetry of the complex, generating (EtO)Zr(MesNP^{i}Pr$_2$)$_3$Co(OEt) (**17**). By using 0.5 equivalents of the peroxide, or by using the bulkier di-*tert*-butyl peroxide, a single alkoxy group was added at Zr, resulting in a Zr^{IV}/Co^{0} complex, (RO)Zr(MesNP^{i}Pr$_2$)$_3$Co(N$_2$) (R = Et (**18^{Et}**), ^{t}Bu (**18^{tBu}**)). Therefore, peroxide O–O bond cleavage proceeds through a one-electron process, whereas S–S and S–H bond activation processes appear to proceed through concerted two-electron redox processes. One-electron oxidation products analogous to **18^{R}** were also obtained through the addition of alcohols or H_2O to **5**.[121]

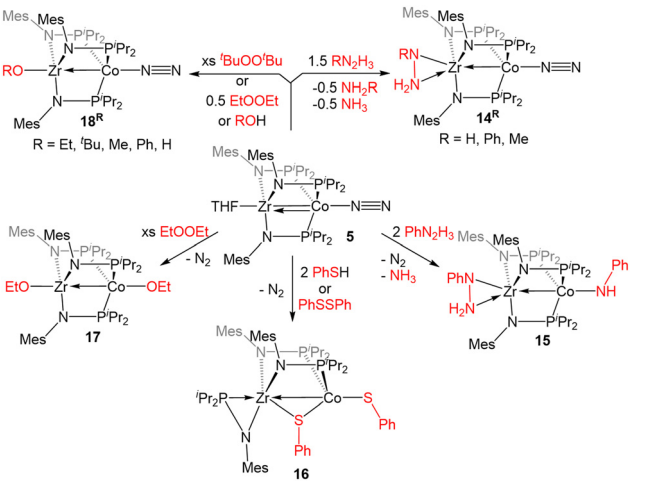

Scheme 3 Examples of E–E and E–H bond activation promoted by **5** (E = N, O, S).

Activation of carbon–heteroatom double bonds. The large differences in the electronegativity of the metal centers in early/late heterobimetallic compounds and the resulting highly polar metal–metal multiple bonds render tris(phosphinoamide) Zr^{IV}/Co^{-I} complexes uniquely suited for activation of polar C=E double bonds (E = N, O, S).

Our first foray into C=E bond activation was the discovery that the Zr^{IV}/Co^{-I} heterobimetallic complex **7** readily cleaved the C=O bond of carbon dioxide (Scheme 4). Exposure of **7** to one equivalent of CO_2 at low temperature resulted in oxidative addition of a C=O double bond across the Zr–Co bond with concomittant dissociation of one of the phosphinoamide ligands from Co, generating $(\eta^2\text{-}^i Pr_2PNMes)Zr(\mu\text{-}MesNP^iPr_2)_2(\mu\text{-}O)Co(CO)$ (**19**).[122] Cyclic voltammetry of **19** revealed a reversible redox event at −1.85 V (*vs.* Fc/Fc^+) and subsequent reduction of **19** with 1 equiv. Na/Hg restored the tris(phosphinoamide) core and afforded the Co^0/Zr^{IV}-oxo anion $[(THF)_3Na][(O)Zr(MesNP^iPr_2)_3Co(CO)]$ (**20**).[122] Using excess Na/Hg to reduce **19** in the presence of an additional equivalent of CO_2 gave a mixture of products, including the carbonate complex $[(THF)_2Na]_2[(CO_3)Zr(MesNP^iPr_2)_3Co(CO)]$ (**21**).[122] Lastly, reaction of **19** with $PhSiH_3$ resulted in the formation of $(PhH_2SiO)Zr(MesNP^iPr_2)_3Co(H)(CO)$ (**22**) *via* cleavage of an Si–H bond across the Co–O bond and reassociation of the third phosphinoamide ligand with Co (Scheme 4).[122] Subsequent studies further explored the fundamental reaction steps involved in CO_2 reduction and carbonate formation using heterobimetallic Zr/Co systems, but realization of a catalytic cycle for CO_2 reduction/functionalization was hindered by the harsh conditions required to cleave Zr–O bonds once formed.[123]

Inspired by the cleavage of C=O bonds in CO_2, the reactivity of **5** with diaryl ketones was investigated (Scheme 5). Benzophenone and its derivatives react with **5** at room temperature to give Zr^{IV}/Co^0 complexes with a ketyl radical bound at Zr *via* single-electron transfer from Co to the Zr-bound ketone.[124–126] In solution, the benzophenone product $(Ph_2C^{\bullet}O)Zr(MesNP^iPr_2)_3CoN_2$ (**23**) was found to be in equilibrium with an isobenzopinacol-coupled tetrametallic product **24**, in which dimerization has occurred through the *para* position of the aryl ring of one Zr/Co complex and the ketyl carbon of a second equivalent of **23**.[124,127] In the case of *para*-methyl benzophenone or fluorenone derivatives, dimerization of the Zr-bound ketyl radical does not occur and the monomeric ketyl radical species can be isolated and structurally characterized. However, placing an electron-donating dimethylamino group at the *para* position results in no electron-transfer or activation of the C=O double bond, with formation of a Zr^{IV}/Co^{-I} ketone adduct instead.[125,126] Ketyl radical species such as **23** were proposed as key intermediates in the catalytic hydrosilylation of ketones performed by **5**.[124] Upon heating the equilibrium mixture of **23** and **24**, the ketone C=O double bond was cleaved in a similar fashion to CO_2 to afford the μ-oxo/carbene complex $(\eta^2\text{-}MesNP^iPr_2)Zr(\mu\text{-}MesNP^iPr_2)_2(\mu\text{-}O)Co{=}CPh_2$ (**25**) in 80% yield, with concomitant formation of a byproduct resulting from cleavage of the phosphinoamide P–N bond.[128]

An analogous reaction with thiobenzophenone, however, led to the partial activation of the C=S bond to generate a product with a $\mu\text{-}\kappa^1\eta^2$ binding mode of the thione (**26**, Scheme 6).[125] The elongation of the C–S bond and the pyrami-

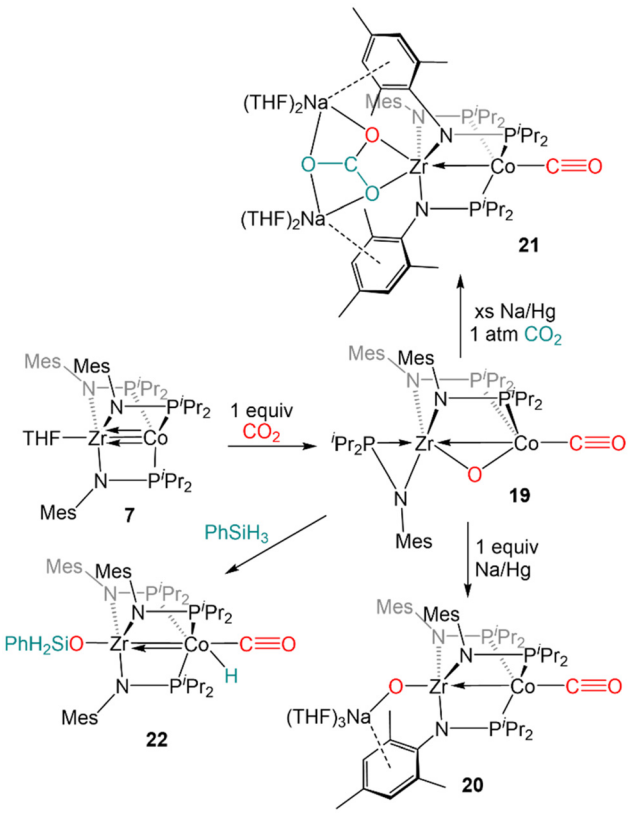

Scheme 4 CO_2 reduction reactions promoted by **7**.

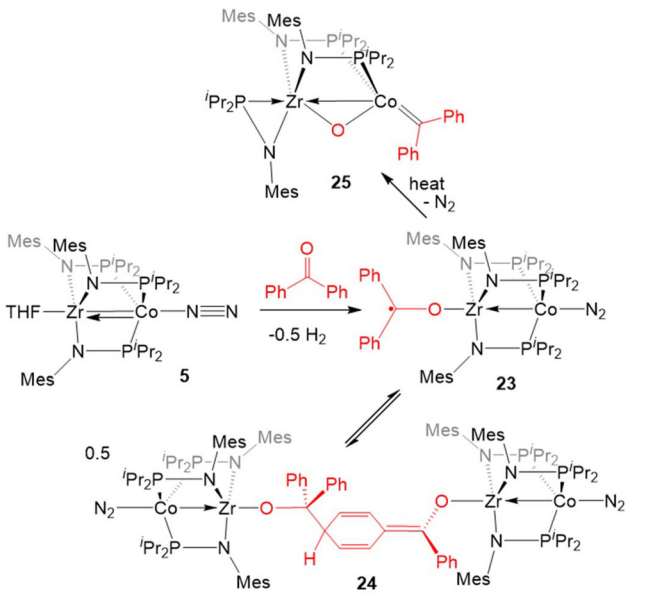

Scheme 5 Reactions of **5** with ketones.

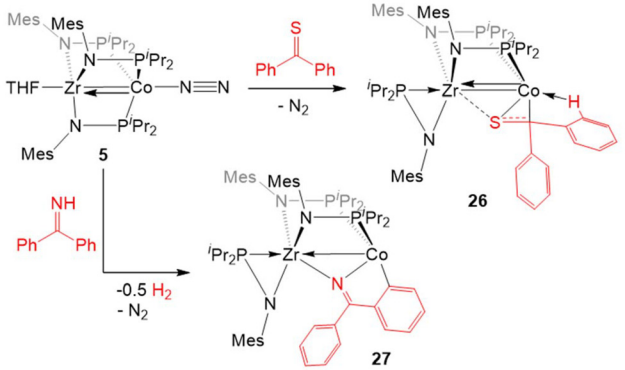

Scheme 6 Representative reactions of **5** with diaryl thioketones and imines.

dalization of the thioketone carbon in **26** provide evidence for the activation of the substrate upon binding across the two metal centers, but a short Zr–Co bond distance (2.3857(2) Å; FSR = 0.91) and the diamagnetic nature of the compound suggest that **26** is best described as a Zr^{IV}/Co^{-I} adduct of thiobenzophenone.

The reaction of **5** with benzophenone imine gave an entirely different result. Rather than cleaving the C=N bond, both N–H and C–H activation occurred to generate a product in which the deprotonated imine is bridging Zr and Co and a 5-membered ring is formed through *ortho*-C–H activation of one of the imine-derived phenyl rings (**27**, Scheme 6).[125] The proposed reaction pathway includes the oxidative addition of the imine N–H bond to form a putative cobalt hydride, which is then lost as dihydrogen in the subsequent cyclometallation of the imine phenyl substituent.[125] In support of such a reaction sequence, addition of fluorenoneimine to **5** generates an isolable hydride species from which cyclometallation is prevented due to the rigidity of the fused arene rings.

Reactivity with oxidative group/atom transfer reagents. The oxidative chemistry of the tris(phosphinoamide) Zr^{IV}/Co^{-I} heterobimetallic systems is not limited to the one- and two-electron oxidative processes described above. In reactions between **6** and organic azides, an overall four-electron redox process was observed (Scheme 7). The treatment of **6** with two equivalents of *p*-tolyl azide resulted in the formation of the Zr^{IV}/Co^{III} compound TolN≡Zr(^{i}PrNP^{i}Pr$_2$)$_3$Co≡NTol (**28**, Tol = *p*-tolyl) *via* oxidative nitrene transfer.[129] This zwitterionic bimetallic compound features a triply bound imido ligand at each C_3-symmetric metal center and no metal–metal interaction (Zr–Co distance = 3.1734(3) Å, FSR = 1.21). Alternatively, addition of the bulkier mesityl azide to **6** produced a diimido species (η^2-^{i}PrNP^{i}Pr$_2$)Zr(μ-^{i}PrNP^{i}Pr$_2$)$_2$(μ-NMes)Co≡NMes with one of the imido ligands bridging the Zr and Co centers and one of the phosphinoamide ligands dissociated from Co and bound η^2 to Zr (**29**).[129] Alkyl azides are notably less reactive than their aryl counterparts,[130] and that trend was also observed in their reactivity with the bimetallic system. While dinitrogen was easily extruded from aryl azides, *tert*-butyl azide reacted with **6** to form (η^2-^{i}PrNP^{i}Pr$_2$)Zr(μ-^{i}PrNP^{i}Pr$_2$)$_2$(μ_2-κ^1,η^3-N^{t}Bu)Co (**30**).[129]

Complex **5** is also reactive towards oxidative O atom transfer from pyridine N-oxide (Scheme 8). Treatment of **5** with pyridine N-oxide affords the bridging oxo complex, (η^2-MesNP^{i}Pr$_2$)Zr(μ-MesNP^{i}Pr$_2$)$_2$(μ-O)Co(py) (**31**, py = pyridine), with pyridine displacing dinitrogen at the apical cobalt site and one phosphinoamide ligand dissociated from Co. In a reaction similar to that of the CO_2 activation product **19** described above, the bridging oxo ligand in **31** was converted to a Zr-bound triphenylsiloxide ligand upon addition of Ph_3SiH, affording (Ph_3SiO)Zr(MesNP^{i}Pr$_2$)$_3$Co(H)(N_2) (**32**).[131] In contrast to **22**, the lability of the N_2 ligand on **32** permitted insertion of unsaturated substrates such as PhC≡CH, PhC≡N, and CO_2 into the Co–H bond (*e.g.* **33**, Scheme 8).[131]

Most of the examples of the reactivity of **5**–**7** provided so far involve the dissociation of the dinitrogen ligand to allow for reactivity at the Co center. Replacement of the labile dinitrogen ligand with ^{t}BuNC, which is sterically bulky and binds more tightly than N_2, gives the Zr^{IV}/Co^{-I} complex (THF)Zr(MesNP^{i}Pr$_2$)$_3$Co(CN^{t}Bu) (**34**), where the coordination sphere about Co remains saturated, forcing substrate coordination to occur at Zr (Scheme 9). Although Zr^{IV} is d^0 and redox inert, the appended Co^{-I} center allows redox processes to occur. In this

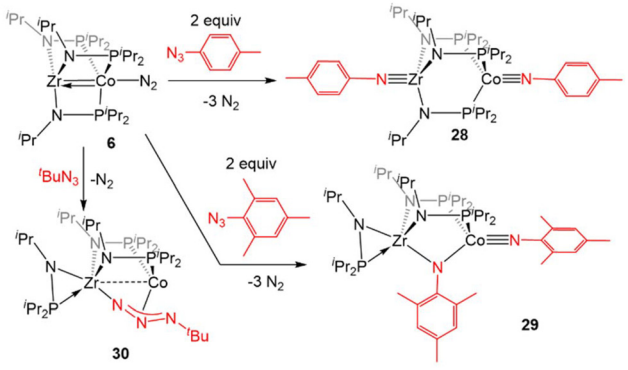

Scheme 7 Reactions between **6** and organic azides.

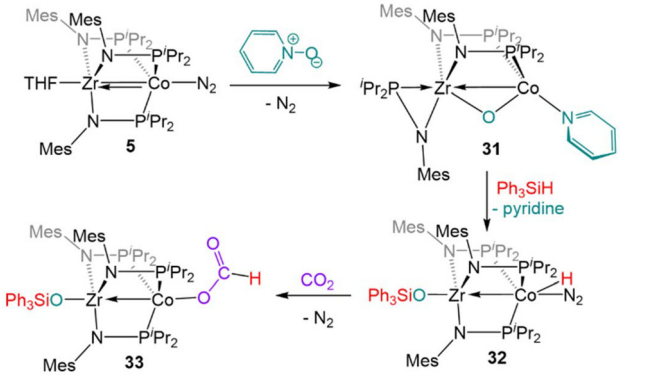

Scheme 8 The two-electron oxidation of **5** with pyridine-N-oxide, subsequent reaction with silane to generate a Zr^{IV}/Co^{I} hydride complex, and a representative insertion reaction with CO_2.

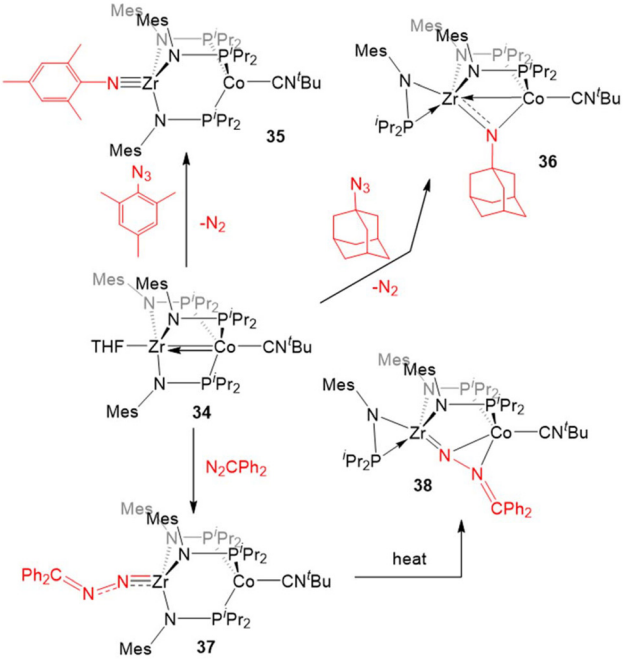

Scheme 9 Examples of two-electron reactions promoted by **34**.

case, it is useful to consider complexes such as **34** as Zr^{IV} complexes with a redox-active Co^{-I} containing metalloligand.[132]

The "redox-active metalloligand" approach is best exemplified in reactions between **34** and oxidative group transfer reagents. As shown in Scheme 9, the addition of mesityl azide to **34**, resulted in the formation of the terminal Zr-imido complex MesN≡Zr(MesNP^{i}Pr$_2$)$_3$Co(CN^{t}Bu) (**35**). The bulkier adamantyl azide instead formed the bridging imido complex (η^2-^{i}Pr$_2$PNMes)Zr(μ-MesNP^{i}Pr$_2$)$_2$(μ-NMes)Co(CN^{t}Bu) (**36**). In both of these cases, two-electron processes were observed, which differs from the previously discussed reactions of organic azides with **6** (Scheme 7, *vide supra*), and shows the ability of *tert*-butyl isocyanide to partially "block" the late metal site.[129,132] Diphenyl diazomethane reacts readily with **34** to form a Zr^{IV}/Co^{I} alkylidene hydrazido complex (Ph$_2$CN$_2$)Zr(MesNP^{i}Pr$_2$)$_3$Co(CN^{t}Bu) (**37**), wherein oxidation of the diazo reagent and formation of a Zr–N multiple bond results in cleavage of the metal–metal bond. Heating of **37** in an effort to promote N_2 release resulted in isomerization to (η^2-^{i}Pr$_2$PNMes)Zr(μ-MesNP^{i}Pr$_2$)$_2$(μ-N$_2$CPh$_2$)Co(CN^{t}Bu) (**38**).[132]

Due to the oxophilic nature of the Zr^{IV} center, the reducing nature of the Co^{-I} center, and the stability of the complex imparted by both the bridging phosphinoamide ligands and the appended isocyanide moiety, **34** was uniquely suited to participate in reactions with O_2 and O-atom donors (Scheme 10). Exposure of **34** to excess dry O_2 resulted in a cobalt-centered two-electron oxidation and binding of the resulting η^2-O_2^{2-} ligand at Zr to generate the Zr^{IV}/Co^{I} compound (η^2-O$_2$)Zr(MesNP^{i}Pr$_2$)$_3$Co(CN^{t}Bu) (**39**).[133]

In contrast to the reaction of **5** with pyridine-N-oxide, the addition of pyridine-N-oxide to **34** afforded the terminal Zr oxo

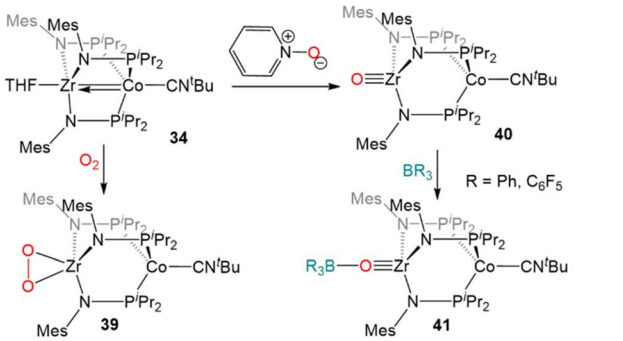

Scheme 10 Two-electron oxidation of **34** using O_2 or pyridine-N-oxide and subsequent nucleophilic reactivity of terminal Zr oxo complex **40**.

complex O≡Zr(MesNP^{i}Pr$_2$)$_3$Co(CN^{t}Bu) (**40**).[133] The isolation of **40** is notable as only one other neutral terminal Zr oxo compound had been previously isolated.[134] The nucleophilicity of the oxo moiety in **40** was confirmed by its ability to readily bind Lewis acidic boranes to generate (R$_3$BO)Zr(MesNP^{i}Pr$_2$)$_3$Co(CN^{t}Bu) (**41**, Scheme 10).[133]

The combination of the nucleophilicity of the Zr-oxo fragment and the redox activity of the appended Co^{I} center opens new avenues for bimetallic cooperativity and the redox properties and further reactivity of **40** were, therefore, investigated (Scheme 11). The Zr^{IV}/Co^{I} oxo complex displays a reversible one-electron reduction at −1.71 V in its cyclic voltammogram, and could be reduced by the addition of Na/Hg amalgam to give the Zr^{IV}/Co^{0} tetrametallic dimer Na$_2$[O≡Zr(MesNP^{i}Pr$_2$)$_3$Co(CN^{t}Bu)]$_2$ (**42**).[135] Another Zr^{IV}/Co^{0} complex (Ph$_3$CO)Zr(MesNP^{i}Pr$_2$)$_3$Co(CN^{t}Bu) (**43**) could be generated by the treatment of **40** with Gomberg's dimer, a source of the trityl radical.[135,136] However, the trityl radical alone is not sufficiently reducing to generate the Co^{0} center present in **43**, so its formation was hypothesized to be driven by the affinity

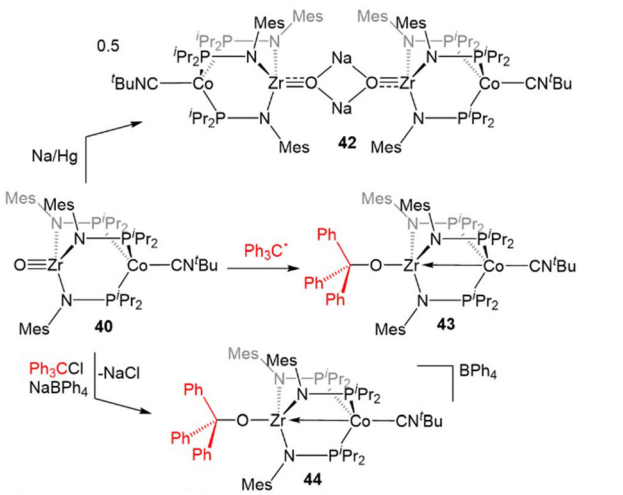

Scheme 11 Reactivity of the Zr-oxo complex **40**.

of the Zr oxo for the trityl cation. Treatment of **40** with Ph_3CCl in the presence of $NaBPh_4$ supported this hypothesis, as the cationic complex $[(Ph_3CO)Zr(MesNP^iPr_2)_3Co(CN^tBu)][BPh_4]$ (**44**) was generated.[135] These reactions serve to highlight a unique example of bimetallic cooperativity in which one transition metal serves as a redox-active electron reservoir while new bonds are formed with a nucleophilic ligand bound to a second redox-inert metal.

Ti/Co and Hf/Co tris(phosphinoamide) complexes

Ti/Co tris(phosphinoamide) complexes

Naturally, there are multiple similarities and subtle differences between the Zr-containing heterobimetallic compounds and their Ti/Co congeners. Most notably, due to the 0.13 Å decrease in atomic radius while moving up group IV to Ti,[28] three mesityl-substituted phosphinoamide ligands cannot be coordinated to the metal center. As such, all comparative studies with Ti/Co tris(phosphinoamide) complexes were carried out using the smaller $[XylNP^iPr_2]^-$ ligand (Xyl = 3,5-dimethylphenyl), necessitating the synthesis of a direct Zr/Co analogue, $(THF)Zr(XylNP^iPr_2)_3CoN_2$ (**45**) (Fig. 8).[137]

The Ti^{IV}/Co^{-I} complex $(THF)Ti(XylNP^iPr_2)_3Co(N_2)$ (**46**) can be synthesized *via* a stepwise metalation/reduction strategy similar to that previously described for the Zr/Co analogue **5**.[138] Exposure to vacuum or preparation in the absence of N_2 affords $(THF)Ti(XylNP^iPr_2)_3Co$ (**47**), a direct analogue of **7**. Similar to its heavier congener,[111] the Ti–Co bond in **47** consists of one σ and two π bonding orbitals with two Co-centered non-bonding orbitals of δ symmetry. N_2 binding in **46** results in elongation of the metal–metal bond by ~0.21 Å, indicative of a decrease in metal–metal bond order.[138] The metal–metal distances in **46** and **47** are shorter than the corresponding distances in **45** and **7** but, owing to the smaller size of Ti, the FSRs are nearly identical (Fig. 8). Through computational studies, the Ti–Co multiple bonds in **46** and **47** were found to be more covalent than the Zr–Co multiple bonds in **5** and **7**, as expected based on better overlap between the 3d orbitals of Ti and Co compared to the 4d/3d overlap in the Zr/Co congeners. This subtle difference in metal–metal bonding manifests in a large difference in the degree of backbonding to N_2 in **45** and **46**. By analyzing the N_2 stretching frequencies by IR spectroscopy, the Ti/Co complex **46** was found to have a markedly less activated N_2 moiety in comparison to its Zr analogue **45** (2084 *vs.* 2045 cm^{-1}, respectively), indicating that Ti–Co bonding withdraws significantly more electron density from the Co center.

The reactivity of **46** was investigated, with the goal of comparing its reactivity patterns with those of **5** (Scheme 12). In this pursuit, **46** and **47** were found to readily react with diaryl ketones to form adducts at either Ti or Co.[126] Addition of one equivalent of benzophenone to **46** affords the Ti-bound ketone adduct $(Ph_2C{=}O)Ti(XylNP^iPr_2)_3Co(N_2)$ (**48**). In solution, **48** was found to be in equilibrium with $(\eta^2\text{-}XylNP^iPr_2)Zr(\mu\text{-}XylNP^iPr_2)_2Co(\eta^2\text{-}O{=}CPh_2)$ (**49**), in which N_2 and one of the phosphinoamide ligands has dissociated from Co allowing benzophenone to bind to Co in an η^2 fashion. Product **49** was formed exclusively when the benzophenone addition reaction was performed under an argon atmosphere. Unlike the reaction of **5** with benzophenone, no evidence for ketyl radical formation was observed and thermolysis did not afford an oxo/carbene complex.[128]

In another example of reactivity that diverges between Zr/Co and Ti/Co combinations, **46** was treated with both hydrazine and methyl hydrazine. While hydrazine was found to undergo one-electron reduction and spontaneous liberation of H_2 upon reaction with Zr^{IV}/Co^{-I} complex **5** (*vide supra*, Scheme 3),[120] the reaction between **46** and hydrazine generates a diamagnetic Ti^{IV}/Co^{-I} ammonia complex $(H_3N)Ti(XylNP^iPr_2)_3Co(N_2)$ (**50**).[138] With methyl hydrazine, **50** and the analogous methylamine complex (**51**) are generated in a 1 : 3 ratio (Scheme 12). In both cases, the reaction is balanced *via* the formation of N_2. Exposure of **46** to a 50-fold excess of hydrazine resulted in catalytic disproportionation of hydrazine into ammonia and dinitrogen with a maximum of 18 turnovers in 30 minutes.[138] In an attempt to generate a model complex that may give infor-

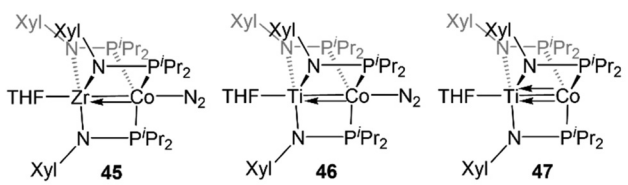

	45	46	47
M-Co distance (Å)	2.3816(10)	2.2320(6)	2.0262(10)
FSR[a]	0.91	0.90	0.82
$\nu(N_2)$ (cm^{-1})	2045	2084	n/a

Fig. 8 A comparison of the metal–metal bond metrics and $\nu(N_2)$ stretching frequencies of Zr^{IV}/Co^{-I} and Ti^{IV}/Co^{-I} complexes. [a] FSR is defined as the ratio of the metal–metal distance to the sum of the single bond atomic radii of the two metals.

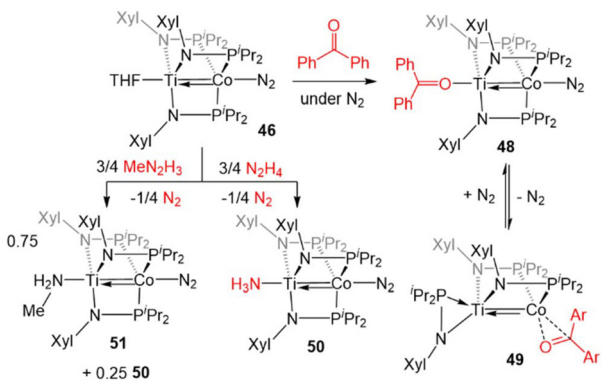

Scheme 12 Examples of the divergent reactivity of Ti^{IV}/Co^{-I} compound **46** compared to Zr^{IV}/Co^{-I} compound **5**.

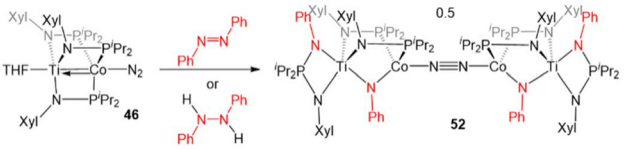

Scheme 13 N–N bond cleavage reaction of Ti^{IV}/Co^{-I} compound **46**.

mation about the catalytically relevant intermediates in N–N bond cleavage, azobenzene was added to **46**, resulting in the cleavage of the N=N double bond, imido insertion into the Co–P bond, formation of a bridging imido ligand, and dimerization of the compound into an N_2-bridged, tetrametallic complex (**52**) (Scheme 13). Product **52** is also generated in the reaction of **46** with 1,2-diphenylhydrazine.[138] Although **52** likely represents a model of an off-cycle product, its isolation indicates that both Ti and Co play an essential role in the disproportionation of hydrazine. The differences in reactivity between the Ti/Co compounds and their Zr/Co analogues are likely due to the increased covalency of the Ti–Co bond and the resulting more positive reduction potential of the Ti/Co compounds.[126]

Hf/Co tris(phosphinoamide) complexes

Despite the nearly identical atomic radii of Zr and Hf and their similar coordination chemistry, tris(phosphinoamide) Hf/Co complexes displayed distinct reactivity from their Zr/Co analogues. A series of Hf^{IV}/Co^{I} precursors, $ClHf(R'NPR_2)_3CoI$ (R′ = ^{i}Pr, R = Ph (**53**); R′ = Mes, R = ^{i}Pr (**54**); R′ = R = ^{i}Pr (**55**)) were synthesized in an identical manner to their Zr analogues (Fig. 9).[112] In comparison to the Zr compounds (Fig. 5) the Hf^{IV}/Co^{I} complexes **53–55** exhibited slightly elongated M–Co bonds and slightly more negative reduction potentials, with the exception of **55**, which exhibits more positive $Co^{I/0}$ and $Co^{0/-I}$ potentials (Fig. 9). Both the longer M–Co distances and cathodically shifted reduction potentials were ascribed to weaker Co→M dative bonds in the Hf/Co compounds, which is expected based on the larger disparity in orbital energies between a 3d and 5d metal compared to a 3d/4d combination.

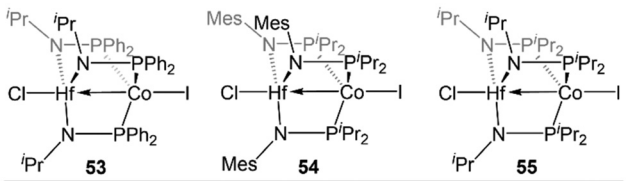

	53	54	55
Hf-Co distance (Å)	2.7548(5)	2.6839(5)	2.6370(7)
FSR[a]	1.06 (Hf) 1.04 (Zr)	1.03 (Hf) 1.00 (Zr)	1.01 (Hf) 1.00 (Zr)
$Co^{I/0}$, *E* (V vs Fc)[b]	-1.66 (Hf) -1.65 (Zr)	-1.69 (Hf) -1.64 (Zr)	-1.79 (Hf) -1.86 (Zr)
$Co^{0/-I}$, *E* (V vs Fc)[b]	≥ -1.66 (Hf) ≥ -1.65 (Zr)	-1.98 (Hf) -1.87 (Zr)	-1.98 (Hf) -2.07 (Zr)

Fig. 9 A comparison of the metal–metal bond metrics and redox potentials of tris(phosphinoamide) Hf^{IV}/Co^{I} and Zr^{IV}/Co^{I} complexes. [a] FSR is defined as the ratio of the metal–metal distance to the sum of the single bond atomic radii of the two metals. [b] The listed potentials represent either $E_{1/2}$ or E_{pc} values, depending on the reversibility of the redox events, but reversibility was consistent between Hf and Zr derivatives.

While the differences in the structural and redox properties of otherwise analogous Zr/Co and Hf/Co complexes were subtle, more tangible differences were observed in the reduced M^{IV}/Co^{-I} species (Fig. 10). Reduction of **53** and **55** results in the formation of Hf^{IV}/Co^{-I} dinitrogen complexes [{ClHf(^{i}PrNPPh$_2$)$_3$CoN$_2$}$_2$Na(THF)$_4$][Na(THF)$_6$] (**56**) and Hf(^{i}PrNP^{i}Pr$_2$)$_3$Co(N$_2$) (**57**),[112] which adopt structures analogous to their Zr^{IV}/Co^{-I} congeners.[111] Upon reduction of **54**, a dinitrogen complex is generated, but the halide ligand remains bound at the Hf site to afford (THF)$_5$Na–X–Hf(MesNP^{i}Pr$_2$)$_3$Co(N$_2$) (**58**).[112] Unlike a similar intermediate generated in the synthesis of **5**,[110] dissolution in benzene does not liberate the sodium halide. The short Hf–Co distances in **56** (2.5470(3) Å, FSR = 0.98) and **58** (2.455(5) Å, FSR = 0.94) are indicative of metal–metal bonds, and their FSRs are greater than that in the Zr complex (THF)$_5$Na–X–Zr(MesNP^{i}Pr$_2$)$_3$Co(N$_2$) (**59**, FSR = 0.92).[110,112] A way to indirectly measure the electron density at the Co center in these compounds is by examination of the IR stretching frequencies of the apically coordinated dinitrogen ligand. The N–N stretches in **56** (2010 cm^{-1}), **58** (1992 cm^{-1}), and **57** (2046 cm^{-1}) are consistently lower than those in the closely related Zr complexes **4** (2015 cm^{-1}), **59** (2023 cm^{-1}), and **6** (2056 cm^{-1}).[110–112] The relatively long intermetallic distances in **56** and **58** suggests that the metal–metal interactions

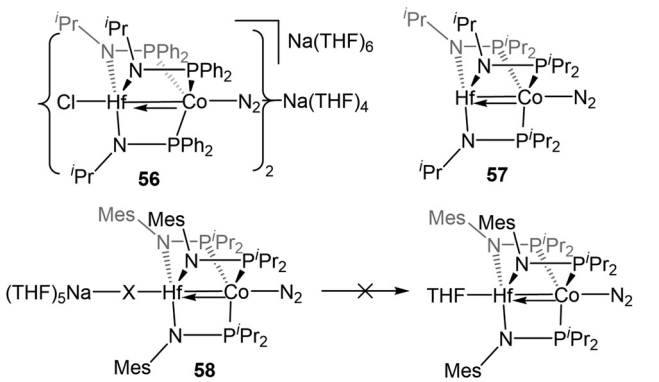

	56	58	57
Hf-Co distance (Å)	2.5470(3)	2.455(5)	n/a
FSR[a]	0.98 (Hf)	0.94 (Hf) 0.92 (Zr)	n/a (Hf) 0.89 (Zr)
$\nu(N_2)$ (cm^{-1})	2010 (Hf) 2015 (Zr)	1992 (Hf) 2023 (Zr)	2046 (Hf) 2056 (Zr)

Fig. 10 A comparison of the metal–metal bond distances and infrared N_2 stretching frequencies of tris(phosphinoamide) Hf^{IV}/Co^{-I} and Zr^{IV}/Co^{-I} complexes. [a] FSR is defined as the ratio of the metal–metal distance to the sum of the single bond atomic radii of the two metals.

in the Hf/Co complexes are weaker than those in their Zr/Co analogues, likely resulting from the decreased bond covalency owing to the energetic mismatch between the Hf and Co d orbitals. This results in a more electron-rich cobalt center in the Hf/Co complexes, which is exemplified by the increased backbonding to the apical dinitrogen ligands in **56–58** compared to their Zr/Co analogues. Decreased Co→Hf donation renders the early metal center more Lewis acidic, accounting for the decreased halide lability in **58**.

Studies of the further reactivity of the Hf/Co compounds revealed stark differences from the Zr/Co analogues but was limited to the mesityl-substituted amide complexes **54** and **58**. As shown in Scheme 14, the exposure of **58** to stoichiometric methyl iodide results in the one-electron oxidation of the complex to form XHf(MesNP^{i}Pr$_2$)$_3$Co(N$_2$) (**60**),[112] in contrast to the two-electron oxidation observed after addition of MeI to Zr^{IV}/Co^{-I} complex **5** (Scheme 1, *vide supra*).[115] In a catalytic study, **54** was found to be much less active than its Zr analogue in Kumada coupling reactions.[112,116]

M/Co bis(phosphinoamide) complexes (M = Ti, Zr)

In studying the reactivity of the group IV/cobalt tris(phosphinoamide) complexes, a common structural pattern was observed: in many two-electron oxidative addition reactions and reactions where substrates are bound to Co in an η^2 fashion, phosphine dissociation from the Co center is required. This results not only in an η^2-phosphinoamide ligand bound at Zr, congesting its coordination sphere, but may contribute to undesirable phosphinoamide degradation reactions that hamper the potential uses of these heterobimetallic complexes in catalysis. Therefore, an alternative bis(phosphinoamide) ligand scaffold was developed to target more coordinatively unsaturated heterobimetallic complexes. These endeavors were successful and both Ti/Co and Zr/Co bis(phosphinoamide) complexes were synthesized. A similar degree of metal–metal multiple bonding was observed with just two buttressing ligands, but the reactivity of the bis(phosphinoamide) compounds was found to be significantly enhanced.

Ti/Co bis(phosphinoamide) complexes

The combination of the Ti^{IV} metalloligand Cl$_2$Ti(XylNP^{i}Pr$_2$)$_2$ with CoI$_2$ in the presence of Zn powder yields the tetrametallic dimer [ClTi(XylNP^{i}Pr$_2$)$_2$CoI]$_2$ (**61**, Scheme 15).[139] Unlike the

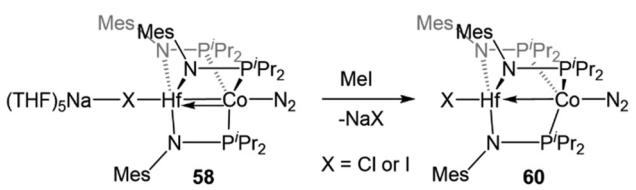

Scheme 14 One-electron oxidation of Hf^{IV}/Co^{-I} complex **58** with MeI, illustrating divergent reactivity compared to the Zr^{IV}/Co^{-I} analogue (*cf.* Scheme 1).

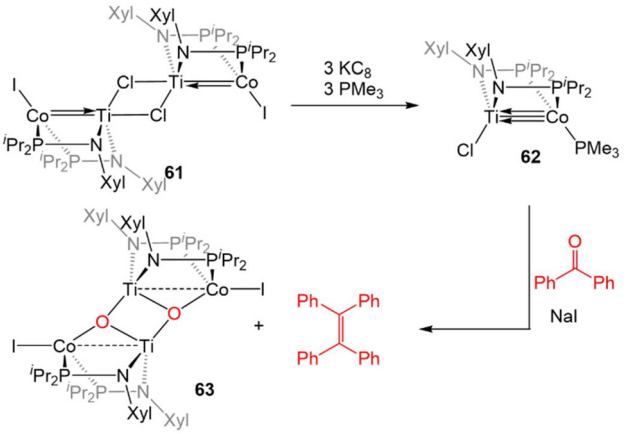

Scheme 15 Synthesis of a bis(phosphinoamide) Ti^{IV}/Co^{-I} complex and its reactivity in a stoichiometric McMurray coupling reaction with benzophenone.

M^{IV}/Co^{I} precursors observed in the tris(phosphinoamide) system, this is a Ti^{IV}/Co^{0} complex and its 2.2051(4) Å intermetallic distance is indicative of a Ti–Co double bond (FSR = 0.89).[139] Furthermore, an examination of the frontier molecular orbitals shows that there is a σ-bonding interaction and two weak π bonding interactions, heavily polarized toward cobalt, between the two metal centers, consistent with a bond order of ~2. Further reduction of **61** with excess KC$_8$ in the presence of PMe$_3$ yields the Ti^{IV}/Co^{-I} complex ClTi(XylNP^{i}Pr$_2$)$_2$Co(PMe$_3$) (**62**). The metal–metal bond in **62** is further contracted to 2.0234(9) Å (FSR = 0.82, Fig. 11) and a computational examination of the frontier molecular orbitals reveals a $(\sigma)^2(\pi)^4(Co_{nb})^4$ electronic configuration consistent with a metal–metal triple bond.[139] The metal–metal distance in **62** is similar to that seen in **47** (2.0262(5) Å; FSR = 0.81), further supporting its assignment as a Ti–Co triple bond.[138]

The highly reduced bimetallic core of **62** reacts readily with aryl ketones in the presence of NaI to give the μ$_3$-oxo dimer [Ti(μ-O)(XylNP^{i}Pr$_2$)$_2$CoI]$_2$ (**63**) and tetraphenylethylene in a stoichiometric McMurray reaction (Scheme 15).[139] This stoichiometric coupling reaction is not observed in the tris(phosphinoamide) Ti/Co complexes, wherein only ketone adducts are observed (Scheme 12, *vide supra*).[126] Due to this vast difference in

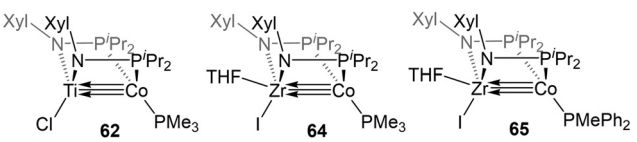

	62	65
M-Co distance (Å)	2.0234(9)	2.2733(6)
FSR[a]	0.82	0.87

Fig. 11 A comparison of the metal–metal bond metrics of bis(phosphinoamide) Ti^{IV}/Co^{-I} and Zr^{IV}/Co^{-I} complexes. [a] FSR is defined as the ratio of the metal–metal distance to the sum of the single bond atomic radii of the two metals.

reactivity, it was concluded that bis(phosphinoamide) complexes are more reactive than their tris(phosphinoamide) analogues.

Zr/Co bis(phosphinoamide) complexes

Bis(phosphinoamide)-linked Zr^{IV}/Co^{-I} compounds, (THF)IZr(XylNP^{i}Pr$_2$)$_2$Co(PR$_3$) (PR$_3$ = PMe$_3$ (**64**), PMePh$_2$ (**65**)), were successfully synthesized and proven even more reactive than bis(phosphinoamide) compound **62** or the aforementioned tris(phosphinoamide) Zr/Co compounds.[140] As shown in Fig. 11, the Zr–Co distance in **65** is 2.2733(6) Å (FSR = 0.87), which is elongated compared to that observed in the N$_2$-free Zr^{IV}/Co^{-I} tris(phosphinoamide) complex **7** (FSR = 0.82) and the Ti^{IV}/Co^{-I} bis(phosphinoamide) analogue **62** (FSR = 0.82).[111,139] As expected, the electronic configuration of **65** was found to be $(\sigma)^2(\pi)^4(Co_{nb})^4$, corresponding to a metal–metal triple bond. However, despite the similar electron configuration, the metal–metal bonding orbitals in **65** were found to be significantly more polarized with far lower Zr contributions, leading to weaker bonding.

The increased polarization and steric accessibility of the metal–metal bond in **64** and **65** renders these complexes significantly more reactive than either their Ti/Co or tris(phosphinoamide) analogues. For example, **64** and **65** react instantaneously and irreversibly with H$_2$ (1 atm) to form the Zr^{IV}/Co^{I} dihydride complex (THF)IZr(μ-H)(XylNP^{i}Pr$_2$)$_2$Co(H)(PR$_3$) (PR$_3$ = PMe$_3$ (**66**), PMePh$_2$ (**67**)) (Scheme 16).[140] This reactivity is in stark contrast to the tris(phosphinoamide) Zr/Co complex **5**, which reacted sluggishly and destructively with H$_2$ over the course of 12 hours to form **11** (Scheme 1; *vide supra*).[115] The Zr–Co distance elongates to 2.4695(3) Å (FSR = 0.94) upon oxidative addition of H$_2$, but remains shorter than observed for previous Zr^{IV}/Co^{I} complexes owing to a three-center–two-electron bond between Zr, Co, and the bridging hydride ligand.[140] Upon exploring the utility of the H$_2$ activation reaction, it was discovered that **64** and **65** are effective catalysts for the semi-hydrogenation of alkynes.[140] At 5 mol% loading of **65** under 1 atm H$_2$ at 60 °C, diphenylacetylene was hydrogenated to a mixture of stilbene isomers with 98% conversion in 6 h (Scheme 16). The PMe$_3$ derivative **64** was also an effective catalyst but was more sluggish, suggesting that phosphine dissociation is a requisite step in the catalytic mechanism. Indeed, phenylacetylene was shown to displace the PMePh$_2$ ligand in **65** to generate (THF)IZr(XylNP^{i}Pr$_2$)$_2$Co(PhCCPh) (**68**) and both **67** and **68** were observed by $^{31}P\{^{1}H\}$ NMR spectroscopy during catalysis. Additionally, independently synthesized **68** was shown to be catalytically competent, with comparable activity to **65** and enhanced activity compared to **64**. In all cases, very little over-hydrogenation occurred (~2% 1,2-diphenylethane), but the stilbene product was generated as a statistical mixture of isomers ($Z:E$ = 57 : 43).[140] Computational investigations of this catalytic cycle suggest that the cleavage of dihydrogen takes place primarily at the cobalt center, with the cleavage of the metal–metal triple bond playing an important role in the formation of the stable bridging hydrides in **66**/**67**.[141] Alkyne insertion then primarily takes place at the terminal cobalt hydride and then reductive elimination occurs, with the Z : E selectivity depending primarily on the steric environment at cobalt.[141]

In addition to the activation of H$_2$, **64** and **65** were also found to activate the C–H bonds of terminal alkynes and pyridine derivatives. In a reaction similar to that described for the tris(phosphinoamide) complex **5** (Scheme 2, *vide supra*), treatment of **65** with TMSC≡CH or PhC≡CH resulted in C$_{sp}$–H oxidative addition to afford a product with a terminal Co-hydride and a bridging acetylide fragment that binds κ^1 to Co and η^2 to Zr (**69** and **70**, Scheme 17).[142] While the tris(phosphinoamide) Zr^{IV}/Co^{-I} complex **5** simply binds pyridine derivatives at the available Zr coordination site,[143] the bis(phosphinoamide) complex **64** undergoes C$_{sp^2}$–H oxidative addition when exposed to pyridine derivatives. For example, the addition of excess 4-methylpyridine to **64** affords the Zr^{IV}/Co^{I} C–H activation product **71** (Scheme 17).[142] The less electron-rich PMePh$_2$-substituted analogue **65**, on the other hand, proved unable to activate the C–H bond of pyridine derivatives, illustrating the delicate steric and electronic influences that dictate the favorability of this reaction. In fact, compound **71** was shown to take part in a dynamic equilibrium in solution through reversible C–H acti-

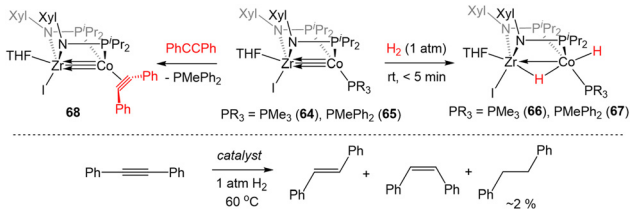

Catalyst	catalyst loading	time (h)	conversion	*Z*:*E*
65	5 mol %	6	99%	56:44
65	10 mol %	3	98%	57:43
64	10 mol %	6	94%	61:39
68	10 mol %	2	93%	69:31

Scheme 16 Reactivity of bis(phosphinoamide) Zr^{IV}/Co^{-I} complexes towards H$_2$ and applications of these compounds as catalysts for the semi-hydrogenation of internal alkynes.

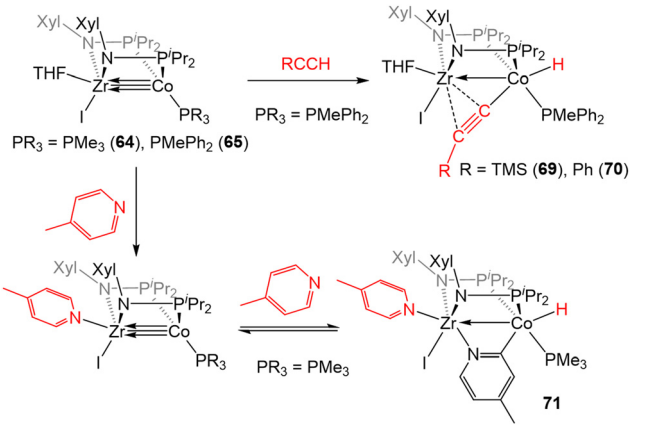

Scheme 17 C–H bond activation promoted by bis(phosphinoamide) Zr^{IV}/Co^{-I} complexes.

vation. The reversibility of the pyridine C–H activation process hampered efforts to promote further C–H functionalization reactions but, nonetheless, this stoichiometric reaction demonstrated the enhanced reactivity of the more coordinatively unsaturated bis(phosphinoamide)supported Zr/Co systems.

Zr/Co mono(phosphinoamide) complexes

The metal–metal bonding in both tris(phosphinoamide)- and bis(phosphinoamide)-supported Zr^{IV}/Co^{-I} complexes is similar, with both ligand frameworks supporting metal–metal triple bonds with remarkably short intermetallic distances (*vide supra*).[111,140] However, the question remained whether the short metal–metal distances are primarily due to the constraints applied on these systems by multiple bridging ligands, or whether metal–metal orbital overlap is the key driving force for the formation of metal–metal multiple bonds. While Casey *et al.* and Bergman *et al.* synthesized Zr^{IV}/group 9 complexes bearing only a single bridging ligand, the group 9 metals in these systems were either in a higher oxidation state or encumbered by multiple π-acidic ligands, hampering the formation of metal–metal multiple bonds.[144,145] Therefore, to understand the unusual stability of phosphinoamide-supported Zr/Co multiple bonds and potentially generate even more reactive species, a mono(phosphinoamide)-supported Zr^{IV}/Co^{-I} complex was targetted.

The tetrametallic mono(phosphinoamide)-bridged Zr^{IV}/Co^{I} precursor $[I_2Zr(\mu\text{-}I)(\mu\text{-}XylNP^iPr_2)CoI]_2$ (**72**) was synthesized and subsequently reduced with KC_8 in the presence of PMe_3 and 18-crown-6 to yield $[(18\text{-crown-6})K][I_3Zr(XylNP^iPr_2)Co(PMe_3)_2]$ (**73**) (Scheme 18).[113] In **73**, the metal–metal distance was found to be 2.170(1) Å (FSR = 0.83), suggesting a high degree of metal–metal multiple bonding with just one bridging phosphinoamide ligand. A DFT analysis of the frontier molecular orbitals of the anionic, chloride analogue of **73** ($\mathbf{73^{Cl}}$) reveals a $(\sigma)^2(\pi)^4(Co_{nb})^4$ electronic configuration (Fig. 12).[113] The Wiberg Bond Index (WBI) and Mayer Bond Order (MBO) of $\mathbf{73^{Cl}}$ were found to be 1.52 and 1.92, respectively. These values are consistent with those of **7** (WBI = 1.49, MBO = 1.73) and **64** (WBI = 1.50, MBO = 1.89), both of which were also found to contain metal–metal triple bonds.[113] This led to the conclusion that the short intermetallic distances are the result of metal–metal multiple bonding rather than constraints imparted by multiple phosphinoamide ligands. Unfortunately, **73** was found to be too reactive to effectively perform stoichiometric or catalytic bond activation reactions.

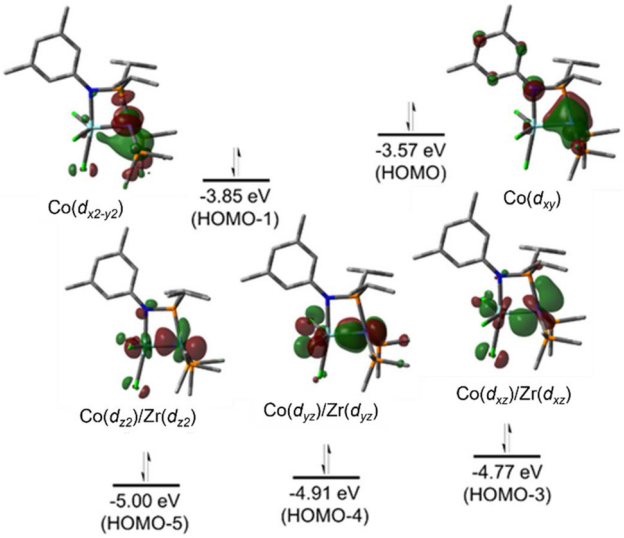

Fig. 12 Pictorial representations of the frontier molecular orbitals of $\mathbf{73^{Cl}}$ (ωB97XD/def2SVP).

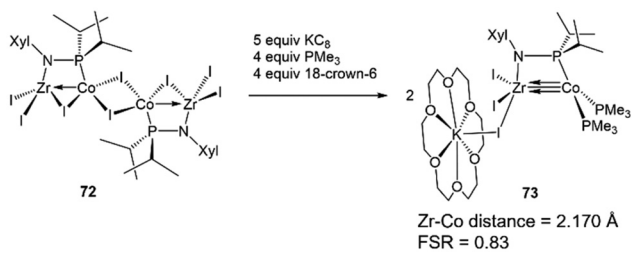

Scheme 18 Synthesis of a mono(phosphinoamide)-supported Zr^{IV}/Co^{-I} complex.

Summary and outlook

An array of phosphinoamide-supported Zr^{IV}/Co^{-I} early/late heterobimetallic complexes have been synthesized and shown to display enhanced redox properties compared to monometallic analogues, polarized metal–metal multiple bonds, and reactivity towards small molecule activation and the cleavage of relatively inert σ and π bonds. The tris(phosphinoamide) ligand scaffold serves as a robust support to study metal–metal multiple bonding and fundamental aspects of the multielectron redox transformations facilitated by Zr/Co complexes. However, oxidative addition reactions across the Zr–Co bond require dissociation of a phosphinoamide ligand from cobalt to allow substrates to access the metal–metal bond. The more coordinatively unsaturated bis(phosphinoamide) complexes can access the same metal–metal multiple bonding motifs as their tris(phosphinoamide) analogues while displaying enhanced reactivity towards inert H–H and C–H bonds. Although a mono(phosphinoamide) Zr^{IV}/Co^{-I} complex was isolated and shown to have comparable metal–metal bonding properties to the bis- and tris(phosphinoamide) analogues, the absence of multiple buttressing ligands rendered this species too unstable for further well-defined reactions. Comparative studies with Ti/Co and Hf/Co complexes indicate that similar metal–metal bonding can be accessed, but that the increased covalency of the Ti–Co bonds and weaker Hf–Co Lewis acid/base interactions leads to diminished reactivity.

The compilation of results described herein suggest that the most promising group IV M/Co (M = Ti, Zr, Hf) complexes

for future reactivity studies are bis(phosphinoamide) Zr/Co compounds. Moreover, the reactivity of these molecules towards inert bonds is likely to be even further enhanced in the absence of strongly binding ancillary ligands (*e.g.* PMe_3) coordinated to the reactive Co^{-I} site. Efforts to realize more reactive Zr^{IV}/Co^{-I} synthons are currently ongoing and will be reported in due course.

Data availability

No primary research results, software or code have been included and no new data were generated or analyzed as part of this review.

Conflicts of interest

There are no conflicts to declare.

Acknowledgements

The research described in this Perspective has been consistently supported by the U.S. Department of Energy, Office of Science, Office of Basic Energy Sciences, Catalysis Science Program, most recently under Award DE-SC0019179. N. H. H. is grateful for the Dean's Distinguished University Fellowship from the Graduate School at The Ohio State University.

Notes and references

1 M. H. Chisholm, Anything One Can Do, Two Can Do, Too – And It's More Interesting, 2009.
2 P. Buchwalter, J. Rosé and P. Braunstein, *Chem. Rev.*, 2015, **115**, 28–126.
3 A. Chaudhary, A. Singh and R. C. Kamboj, *Chem. Sci. Rev. Lett.*, 2016, **5**, 170–192.
4 J. A. Chipman and J. F. Berry, *Chem. Rev.*, 2020, **120**, 2409–2447.
5 N. P. Mankad, *Chem. – Eur. J.*, 2016, **22**, 5822–5829.
6 M. K. Karunananda and N. P. Mankad, *ACS Catal.*, 2017, **7**, 6110–6119.
7 D. R. Pye and N. P. Mankad, *Chem. Sci.*, 2017, **8**, 1705–1718.
8 C. M. Farley and C. Uyeda, *Trends Chem.*, 2019, **1**, 497–509.
9 I. G. Powers and C. Uyeda, *ACS Catal.*, 2017, **7**, 936–958.
10 B. G. Cooper, J. W. Napoline and C. M. Thomas, *Catal. Rev.: Sci. Eng.*, 2012, **54**, 1–40.
11 P. A. Lindahl, *J. Inorg. Biochem.*, 2012, **106**, 172–178.
12 M. Can, F. A. Armstrong and S. W. Ragsdale, *Chem. Rev.*, 2014, **114**, 4149–4174.
13 J. C. Fontecilla-Camps, A. Volbeda, C. Cavazza and Y. Nicolet, *Chem. Rev.*, 2007, **107**, 4273–4303.
14 M. H. Baik, M. Newcomb, R. A. Friesner and S. J. Lippard, *Chem. Rev.*, 2003, **103**, 2385–2419.
15 E. I. Solomon, T. C. Brunold, M. I. Davis, J. N. Kemsley, S.-K. Lee, N. Lehnert, F. Neese, A. J. Skulan, Y.-S. Yang and J. Zhou, *Chem. Rev.*, 2000, **100**, 235–350.
16 J. J. H. B. Sattler, J. Ruiz-Martinez, E. Santillan-Jimenez and B. M. Weckhuysen, *Chem. Rev.*, 2014, **114**, 10613–10653.
17 S. J. Tauster, *Acc. Chem. Res.*, 1987, **20**, 389–394.
18 W.-F. Liaw, C.-Y. Chiang, G.-H. Lee, S.-M Peng, C.-H. Lai and M. Y. Darensbourg, *Inorg. Chem.*, 2000, **39**, 480–484.
19 T. Zhao, P. Ghosh, Z. Martinez, X. Liu, X. Meng and M. Y. Darensbourg, *Organometallics*, 2017, **36**, 1822–1827.
20 S. Ding, P. Ghosh, M. Y. Darensbourg and M. B. Hall, *Proc. Natl. Acad. Sci. U. S. A.*, 2017, **114**, E9775–E9782.
21 M. Y. Darensbourg, E. L. Oduaran, S. Ding, A. M. Lunsford, K. D. K. Patherana, P. Ghosh and X. Yang, in *Enzymes for Solving Humankind's Problems*, ed. J. J. G. Moura, I. Moura and L. B. Maia, 2021, pp. 275–302.
22 A. McSkimming and D. L. M. Suess, *Nat. Chem.*, 2021, **13**, 666–670.
23 B. E. Petel and E. M. Matson, *Chem. Commun.*, 2020, **56**, 13477–13490.
24 W. Zhang, C. E. Moore and S. Zhang, *J. Am. Chem. Soc.*, 2022, **144**, 1709–1717.
25 J. A. Kephart, B. S. Mitchell, W. Kaminsky and A. Velian, *J. Am. Chem. Soc.*, 2022, **144**, 9206–9211.
26 F. A. Cotton, C. A. Murillo and R. A. Walton, *Multiple Bonds Between Metal Atoms*, Springer Science and Business Media, Inc., New York, 2005.
27 L. Pauling, *The Nature of the Chemical Bond and the Structure of Molecules and Crystals: An Introduction to Modern Structural Chemistry*, Cornell University Press, Ithaca, NY, 3rd edn, 1960.
28 L. Pauling, *J. Am. Chem. Soc.*, 1947, **69**, 542–553.
29 F. A. Cotton, *Acc. Chem. Res.*, 1978, **11**, 225–232.
30 J. A. Bertrand, F. A. Cotton and W. A. Dollase, *J. Am. Chem. Soc.*, 1963, **85**, 1349–1350.
31 M. J. Bennett, F. A. Cotton and R. A. Walton, *J. Am. Chem. Soc.*, 1966, **88**, 3866–3867.
32 F. A. Cotton, *Inorg. Chem.*, 1965, **4**, 334–336.
33 J. P. Krogman and C. M. Thomas, *Chem. Commun.*, 2014, **50**, 5115–5127.
34 J. E. McGrady, in *Molecular Metal-Metal Bonds*, ed. S. T. Liddle, Wiley-VCH Verlag GmbH & Co. KGaA, Weinheim, Germany, 2015, pp. 1–22.
35 Q. Wang, S. H. Brooks, T. Liu and N. C. Tomson, *Chem. Commun.*, 2021, **57**, 2839–2853.
36 F. G. A. Stone, *Angew. Chem., Int. Ed. Engl.*, 1984, **23**, 89–99.
37 K. M. Baines and W. G. Stibbs, in *Multiply Bonded Main Group Metals and Metalloids*, ed. F. G. A. Stone and R. West, Elsevier Masson SAS, 1st edn, 1996, vol. 39, pp. 275–324.
38 J. P. Collman and R. Boulatov, *Angew. Chem., Int. Ed.*, 2002, **41**, 3948–3961.

39 M. H. Chisholm, *Proc. Natl. Acad. Sci. U. S. A.*, 2007, **104**, 2563–2570.
40 C. Ni and P. P. Power, in *Metal-Metal Bonding*, ed. G. Parkin, Springer Berlin, Heidelberg, 1st edn, 2010, vol. 136, pp. 59–111.
41 G. Parkin, in *Metal-Metal Bonding*, ed. G. Parkin, Springer Berlin Heidelberg, Berlin, Heidelberg, 2010, pp. 113–145.
42 J. F. Berry, in *Metal-Metal Bonding*, ed. G. Parkin, Springer Berlin, Heidelberg, 1st edn, 2010, vol. 136, pp. 1–28.
43 M. H. Chisholm, in *Metal-Metal Bonding*, ed. G. Parkin, Springer Berlin, Heidelberg, 1st edn, 2010, vol. 136, pp. 29–57.
44 T. Nguyen, A. D. Sutton, M. Brynda, J. C. Fettinger, G. J. Long and P. P. Power, *Science*, 2005, **310**, 844–847.
45 L. Pauling, *The Nature of the Chemical Bond*, Cornell University Press, Ithaca, NY, 3rd edn, 1960.
46 F. A. Cotton and M. Millar, *J. Am. Chem. Soc.*, 1977, **99**, 7886–7891.
47 F. A. Cotton, L. M. Daniels and C. A. Murillo, *Angew. Chem., Int. Ed. Engl.*, 1992, **31**, 737–738.
48 F. A. Cotton, L. M. Daniels and C. A. Murillo, *Inorg. Chem.*, 1993, **32**, 2881–2885.
49 P. Berno, S. Hao, R. Minhas and S. Gambarotta, *J. Am. Chem. Soc.*, 1994, **116**, 7417–7418.
50 F. A. Cotton and D. J. Timmons, *Polyhedron*, 1998, **17**, 179–184.
51 F. A. Cotton, E. A. Hillard, C. A. Murillo and X. Wang, *Inorg. Chem.*, 2003, **42**, 6063–6070.
52 F. A. Cotton, E. A. Hillard and C. A. Murillo, *J. Am. Chem. Soc.*, 2003, **125**, 2026–2027.
53 F. A. Cotton, Z. Li and C. A. Murillo, *Eur. J. Inorg. Chem.*, 2007, 3509–3513.
54 J. Haywood, F. A. Stokes, R. J. Less, M. McPartlin, A. E. H. Wheatley and D. S. Wright, *Chem. Commun.*, 2011, **47**, 4120.
55 F. A. Cotton, L. M. Daniels and C. A. Murillo, *Inorg. Chim. Acta*, 1994, **224**, 5–9.
56 G. H. Timmer and J. F. Berry, *C. R. Chim.*, 2012, **15**, 192–201.
57 F. A. Cotton and R. Poli, *Inorg. Chem.*, 1987, **26**, 3652–3653.
58 L. P. He, C. L. Yao, M. Naris, J. C. Lee, J. D. Korp and J. L. Bear, *Inorg. Chem.*, 1992, **31**, 620–625.
59 F. A. Cotton, L. M. Daniels, X. Feng, D. J. Maloney, J. H. Matonic and C. A. Murilio, *Inorg. Chim. Acta*, 1997, **256**, 291–301.
60 F. A. Cotton, Z. Li, C. Murillo, P. Poplaukhin and J. Reibenspies, *J. Cluster Sci.*, 2008, **19**, 89–97.
61 M. Corbett, B. F. Hoskins, N. J. McLeod and B. P. O'Day, *Aust. J. Chem.*, 1975, **28**, 2377–2392.
62 D. I. Arnold, F. A. Cotton, D. J. Maloney, J. H. Matonic and C. A. Murillo, *Polyhedron*, 1997, **16**, 133–141.
63 J. F. Berry, E. Bothe, F. A. Cotton, S. A. Ibragimov, C. A. Murillo, D. Villagrán and X. Wang, *Inorg. Chem.*, 2006, **45**, 4396–4406.
64 K. Pang, J. S. Figueroa, I. A. Tonks, W. Sattler and G. Parkin, *Inorg. Chim. Acta*, 2009, **362**, 4609–4615.
65 T. Hamaguchi, R. Shimazaki and I. Ando, *J. Mol. Struct.*, 2018, **1173**, 345–348.
66 S. O. Ojwach, T. T. Okemwa, N. W. Attandoh and B. Omondi, *Dalton Trans.*, 2013, **42**, 10735.
67 M. Iqbal, I. Ahmad, S. Ali, N. Muhammad, S. Ahmed and M. Sohail, *Polyhedron*, 2013, **50**, 524–531.
68 P. L. Dunn, R. K. Carlson and I. A. Tonks, *Inorg. Chim. Acta*, 2017, **460**, 43–48.
69 J. F. Berry and C. C. Lu, *Inorg. Chem.*, 2017, **56**, 7577–7581.
70 L. M. Slaughter and P. T. Wolczanski, *Chem. Commun.*, 1997, 2109–2110.
71 C. M. Thomas, *Comments Inorg. Chem.*, 2011, **32**, 14–38.
72 R. J. Eisenhart, L. J. Clouston and C. C. Lu, *Acc. Chem. Res.*, 2015, **48**, 2885–2894.
73 N. Wheatley and P. Kalck, *Chem. Rev.*, 1999, **99**, 3379–3419.
74 D. W. Stephan, *Coord. Chem. Rev.*, 1989, **95**, 41–107.
75 R. M. Bullock and C. P. Casey, *Acc. Chem. Res.*, 1987, **20**, 167–173.
76 L. H. Gade, *Angew. Chem., Int. Ed.*, 2000, **39**, 2658–2678.
77 K. Koessler and B. Butschke, *Encyclopedia of Inorganic and Bioinorganic Chemistry*, 2021, pp. 1–31.
78 R. T. K. Baker, S. J. Tauster and J. A. Dumesic, *Strong Metal-Support Interactions*, American Chemical Society, Washington, DC, USA, 1986, vol. 298.
79 S. J. Tauster, *ACS Symp. Ser.*, 1986, **298**, 1–9.
80 S. Friedrich, H. Memmler, L. H. Gade, W. S. Li, I. J. Scowen, M. McPartlin and C. E. Housecroft, *Inorg. Chem.*, 1996, **35**, 2433–2441.
81 G. S. Ferguson and P. T. Wolczanski, *J. Am. Chem. Soc.*, 1986, **108**, 8293–8295.
82 G. S. Ferguson, P. T. Wolczanski, L. Parkanyi and M. C. Zonnevylle, *Organometallics*, 1988, **7**, 1967–1979.
83 G. S. Ferguson and P. T. Wolczanski, *Organometallics*, 1985, **4**, 1601–1605.
84 S. M. Baxter, G. S. Ferguson and P. T. Wolczanski, *J. Am. Chem. Soc.*, 1988, **110**, 4231–4241.
85 P. A. Rudd, S. Liu, L. Gagliardi, V. G. Young and C. C. Lu, *J. Am. Chem. Soc.*, 2011, **133**, 20724–20727.
86 J. T. Moore, S. Chatterjee, M. Tarrago, L. J. Clouston, S. Sproules, E. Bill, V. Bernales, L. Gagliardi, S. Ye, K. M. Lancaster and C. C. Lu, *Inorg. Chem.*, 2019, **58**, 6199–6214.
87 L. J. Clouston, V. Bernales, R. C. Cammarota, R. K. Carlson, E. Bill, L. Gagliardi and C. C. Lu, *Inorg. Chem.*, 2015, **54**, 11669–11679.
88 L. J. Clouston, R. B. Siedschlag, P. A. Rudd, N. Planas, S. Hu, A. D. Miller, L. Gagliardi and C. C. Lu, *J. Am. Chem. Soc.*, 2013, **135**, 13142–13148.
89 R. J. Eisenhart, P. A. Rudd, N. Planas, D. W. Boyce, R. K. Carlson, W. B. Tolman, E. Bill, L. Gagliardi and C. C. Lu, *Inorg. Chem.*, 2015, **54**, 7579–7592.
90 P. A. Rudd, S. Liu, N. Planas, E. Bill, L. Gagliardi and C. C. Lu, *Angew. Chem., Int. Ed.*, 2013, **52**, 4449–4452.

91 R. C. Cammarota, M. V. Vollmer, J. Xie, J. Ye, J. C. Linehan, S. A. Burgess, A. M. Appel, L. Gagliardi and C. C. Lu, *J. Am. Chem. Soc.*, 2017, **139**, 14244–14250.
92 J. Ye, R. C. Cammarota, J. Xie, M. V. Vollmer, D. G. Truhlar, C. J. Cramer, C. C. Lu and L. Gagliardi, *ACS Catal.*, 2018, **8**, 4955–4968.
93 M. V. Vollmer, J. Ye, J. C. Linehan, B. J. Graziano, A. Preston, E. S. Wiedner and C. C. Lu, *ACS Catal.*, 2020, **10**, 2459–2470.
94 B. L. Ramirez, P. Sharma, R. J. Eisenhart, L. Gagliardi and C. C. Lu, *Chem. Sci.*, 2019, **10**, 3375–3384.
95 B. L. Ramirez and C. C. Lu, *J. Am. Chem. Soc.*, 2020, **142**, 5396–5407.
96 J. T. Moore and C. C. Lu, *J. Am. Chem. Soc.*, 2020, **142**, 11641–11646.
97 H. Nagashima, T. Sue, T. Oda, A. Kanemitsu, T. Matsumoto, Y. Motoyama and Y. Sunada, *Organometallics*, 2006, **25**, 1987–1994.
98 H. Tsutsumi, Y. Sunada, Y. Shiota, K. Yoshizawa and H. Nagashima, *Organometallics*, 2009, **28**, 1988–1991.
99 T. Sue, Y. Sunada and H. Nagashima, *Eur. J. Inorg. Chem.*, 2007, 2897–2908.
100 Y. Sunada, T. Sue, T. Matsumoto and H. Nagashima, *J. Organomet. Chem.*, 2006, **691**, 3176–3182.
101 S. Kuppuswamy, M. W. Bezpalko, T. M. Powers, M. J. T. Wilding, C. K. Brozek, M. Foxman and C. M. Thomas, *Chem. Sci.*, 2014, **5**, 1617–1626.
102 S. Kuppuswamy, T. M. Powers, J. P. Krogman, M. W. Bezpalko, B. M. Foxman and C. M. Thomas, *Chem. Sci.*, 2013, **4**, 3557–3565.
103 S. M. Greer, J. McKay, K. M. Gramigna, C. M. Thomas, S. A. Stoian and S. Hill, *Inorg. Chem.*, 2018, **57**, 5870–5878.
104 B. Wu, M. J. T. Wilding, S. Kuppuswamy, M. W. Bezpalko, B. M. Foxman and C. M. Thomas, *Inorg. Chem.*, 2016, **55**, 12137–12148.
105 G. Culcu, D. A. Iovan, J. P. Krogman, M. J. T. Wilding, M. W. Bezpalko, B. M. Foxman and C. M. Thomas, *J. Am. Chem. Soc.*, 2017, **139**, 9627–9636.
106 B. A. Barden, G. Culcu, J. P. Krogman, M. W. Bezpalko, G. P. Hatzis, D. A. Dickie, B. M. Foxman and C. M. Thomas, *Inorg. Chem.*, 2019, **58**, 821–833.
107 D. A. Evers, A. H. Bluestein, B. M. Foxman and C. M. Thomas, *Dalton Trans.*, 2012, **41**, 8111–8115.
108 J. W. Napoline, S. J. Kraft, E. M. Matson, P. E. Fanwick, S. C. Bart and C. M. Thomas, *Inorg. Chem.*, 2013, **52**, 12170–12177.
109 J. P. Krogman, J. R. Gallagher, G. Zhang, A. S. Hock, J. T. Miller and C. M. Thomas, *Dalton Trans.*, 2014, **43**, 13852–13857.
110 B. P. Greenwood, S. I. Forman, G. T. Rowe, C.-H. Chen, B. M. Foxman and C. M. Thomas, *Inorg. Chem.*, 2009, **48**, 6251–6260.
111 B. P. Greenwood, G. T. Rowe, C.-H. Chen, B. M. Foxman and C. M. Thomas, *J. Am. Chem. Soc.*, 2010, **132**, 44–45.
112 V. N. Setty, W. Zhou, B. M. Foxman and C. M. Thomas, *Inorg. Chem.*, 2011, **50**, 4647–4655.
113 N. H. Hunter, J. E. Stevens, C. E. Moore and C. M. Thomas, *Inorg. Chem.*, 2023, **62**, 659–663.
114 X. Yang, L. Zhao, T. Fox, Z.-X. Wang and H. Berke, *Angew. Chem., Int. Ed.*, 2010, **49**, 2058–2062.
115 C. M. Thomas, J. W. Napoline, G. T. Rowe and B. M. Foxman, *Chem. Commun.*, 2010, **46**, 5790–5792.
116 W. Zhou, J. W. Napoline and C. M. Thomas, *Eur. J. Inorg. Chem.*, 2011, 2029–2033.
117 J. Coombs, D. Perry, D.-H. Kwon, C. M. Thomas and D. H. Ess, *Organometallics*, 2018, **37**, 4195–4203.
118 J. W. Beattie, C. Wang, H. Zhang, J. P. Krogman, B. M. Foxman and C. M. Thomas, *Dalton Trans.*, 2020, **49**, 2407–2411.
119 Y. Sun, J. Zhang, Y. Zeng, L. Meng and X. Li, *J. Org. Chem.*, 2024, **89**, 605–616.
120 J. W. Napoline, M. W. Bezpalko, B. M. Foxman and C. M. Thomas, *Chem. Commun.*, 2013, **49**, 4388–4390.
121 J. W. Napoline, J. P. Krogman, R. Shi, S. Kuppuswamy, M. W. Bezpalko, B. M. Foxman and C. M. Thomas, *Eur. J. Inorg. Chem.*, 2013, 3874–3882.
122 J. P. Krogman, B. M. Foxman and C. M. Thomas, *J. Am. Chem. Soc.*, 2011, **133**, 14582–14585.
123 J. P. Krogman, M. W. Bezpalko, B. M. Foxman and C. M. Thomas, *Inorg. Chem.*, 2013, **52**, 3022–3031.
124 W. Zhou, S. L. Marquard, M. W. Bezpalko, B. M. Foxman and C. M. Thomas, *Organometallics*, 2013, **32**, 1766–1772.
125 S. L. Marquard, M. W. Bezpalko, B. M. Foxman and C. M. Thomas, *Organometallics*, 2014, **33**, 2071–2079.
126 H. Zhang, B. Wu, S. L. Marquard, E. D. Litle, D. A. Dickie, M. W. Bezpalko, B. M. Foxman and C. M. Thomas, *Organometallics*, 2017, **36**, 3498–3507.
127 M. P. Crockett, H. Zhang, C. M. Thomas and J. A. Byers, *Chem. Commun.*, 2019, **55**, 14426–14429.
128 S. L. Marquard, M. W. Bezpalko, B. M. Foxman and C. M. Thomas, *J. Am. Chem. Soc.*, 2013, **135**, 6018–6021.
129 B. Wu, R. Hernández Sánchez, M. W. Bezpalko, B. M. Foxman and C. M. Thomas, *Inorg. Chem.*, 2014, **53**, 10021–10023.
130 N. P. Mankad, P. Mueller and J. C. Peters, *J. Am. Chem. Soc.*, 2010, 4083–4085.
131 J. P. Krogman, B. M. Foxman and C. M. Thomas, *Organometallics*, 2015, **34**, 3159–3166.
132 J. P. Krogman, M. W. Bezpalko, B. M. Foxman and C. M. Thomas, *Dalton Trans.*, 2016, **45**, 11182–11190.
133 H. Zhang, G. P. Hatzis, C. E. Moore, D. A. Dickie, M. W. Bezpalko, B. M. Foxman and C. M. Thomas, *J. Am. Chem. Soc.*, 2019, **141**, 9516–9520.
134 W. A. Howard, M. Waters and G. Parkin, *J. Am. Chem. Soc.*, 1993, **115**, 4917–4918.
135 H. Zhang, G. P. Hatzis, D. A. Dickie, C. M. Thomas and C. E. Moore, *Chem. Sci.*, 2020, **11**, 10729–10736.
136 M. Gomberg, *J. Am. Chem. Soc.*, 1903, **25**, 1274–1277.
137 W. Zhou, N. I. Saper, J. P. Krogman, B. M. Foxman and C. M. Thomas, *Dalton Trans.*, 2014, **43**, 1984–1989.
138 B. Wu, K. M. Gramigna, M. W. Bezpalko, B. M. Foxman and C. M. Thomas, *Inorg. Chem.*, 2015, **54**, 10909–10917.

139 B. Wu, M. W. Bezpalko, B. M. Foxman and C. M. Thomas, *Chem. Sci.*, 2015, **6**, 2044–2049.
140 K. M. Gramigna, D. A. Dickie, B. M. Foxman and C. M. Thomas, *ACS Catal.*, 2019, **9**, 3153–3164.
141 Y. Li, P. Su, J. Jiang and Z. Ke, *ACS Catal.*, 2021, **11**, 13452–13462.
142 N. H. Hunter, E. M. Lane, K. M. Gramigna, C. E. Moore and C. M. Thomas, *Organometallics*, 2021, **40**, 3689–3696.
143 B. Crown *thesis*, Brandeis University, 2013..
144 C. P. Casey and F. Nief, *Organometallics*, 1985, **4**, 1218–1220.
145 A. M. Baranger and R. G. Bergman, *J. Am. Chem. Soc.*, 1994, **116**, 3822–3835.